DOE/ER/40633--T1

Final Report

for the

High Energy Physics Program at Texas A&M University

DOE Grant DE-FG05-91ER40633

For the period
April 1, 1995 to March 31, 1996

Department of Physics
Texas A&M University
College Station, Texas 77843

December, 1995

DISCLAIMER

TABLE OF CONTENTS

ABSTRACT

The experimental and theoretical high energy physics programs at Texas A&M University have continued their vigorous research activities over the past year. This is the final report on activities which have been supported through DOE grant DE-FG05-91ER40633. This report covers the period January 1, 1995 to December 31, 1995.

I. The Fermilab Program

The physics program using the Fermilab Tevatron is one of our main research projects. We [1] are members of the Collider Detector (CDF) collaboration at Fermilab. About 80 pb^{-1} data collected with CDF in Run 1B (1994-95) and in addition to the data leading to the discovery of the top quark this running has also provided us with an exciting opportunity to test Supersymmetry (SUSY). With the results on electroweak and strong gauge couplings from CERN's LEP experiments, the models of supersymmetry have become more predictive and require a spectrum of new particles in the mass range of 100-1000 GeV/c^2. Supersymmetry uniquely opens the possibility to directly connect the Standard Model with an ultimate unification of the fundamental interactions. In the past year, our group has led CDF's SUSY searches (see Section A).

In the operation of CDF, our group has provided one person for 'ACE' shifts during many periods of the 1994-95 run. We also coordinate the regular monitoring of the data quality of the gas calorimeters. The gas calorimeter energy scale is particularly important for several analyses which use a missing transverse energy ($\not\!\!E_T$) signature: *e.g.*, W mass measurement. The performance of the gas calorimeters is summarized in Section B.

The upgraded Silicon Vertex detector (SVX-II) is designed to provide a high resolution vertex detection at the high luminosity expected with the Fermilab main injector in 1999. We initiated an idea of five-layer design improving background rejection for both top and b physics analyses. These efforts have led to the five-layer SVX-II being accepted as the baseline design. The progress on these activities is given in Section C.

TeV2000 group was formed to develop a detailed analysis of a possible luminosity upgrade to the Fermilab Tevatron complex, beyond construction of the Main Injector. Dr. Kamon is serving as co-convener of TeV2000 SUSY subgroup. This group has studied the signals and backgrounds for supersymmetric particles at an upgraded Tevatron. A summary report of these activities is given in Section D.

Finally, in Section E, a proposal for our research program for the coming year is presented.

[1] T. Kamon, P. McIntyre, R. Webb (faculty); J. Wolinski (research associate); J.P. Done, J. Lu, B. Tannenbaum (graduate students) in Run 1B (1994-95).

A. CDF Physics Analyses - SUSY[2]

A.1. Search for Chargino-Neutralino Production in Run 1A

Although the Standard Model (SM) provides remarkable agreement with current high energy physics data, it fails to provide insight into several important issues. Among these are the apparently arbitrary energy scale of electro-weak symmetry breaking, the appearance of divergences in the Higgs boson self-energy [1], and the failure of coupling constants to unify at large energy scales [2]. An extension to the SM which may alleviate these difficulties is Supersymmetry (SUSY) [3, 2].

In SUSY, every SM particle is given a SUSY partner with identical quantum numbers but a different spin assignment: fermions get a bosonic partner, bosons receive a fermionic partner. The simplest SUSY extension to the SM is the Minimal Supersymmetric Standard Model (MSSM [4]), which contains four neutral and two charged electro-weak gauge particles (χ's), in addition to the known W and Z gauge bosons. The production cross section for $p\bar{p}\rightarrow\tilde{\chi}_1^{\pm}\tilde{\chi}_2^0$ at $\sqrt{s}$= 1.8 TeV is expected to be O(few) pb [5]. Furthermore, assuming slepton and sneutrino mass constraints [6] motivated by Supergravity (SUGRA) [7] and the GUT hypothesis [8], the leptonic decays $\tilde{\chi}_1^{\pm}\rightarrow\tilde{\chi}_1^0\ell^{\pm}\nu$ and $\tilde{\chi}_2^0\rightarrow\tilde{\chi}_1^0\ell^+\ell^-$ can become appreciable ($\sim$ 20%). The resulting trilepton final state has small SM backgrounds, making it an excellent discovery signature. Consequently, we have searched for $\tilde{\chi}_1^{\pm}\tilde{\chi}_2^0\rightarrow\ell^+\ell^-\ell X$ events and report our findings in this section of our proposal.

The data for this analysis were obtained in $\sqrt{s}$=1.8 TeV $p\bar{p}$ collisions at the Fermilab Tevatron during the 1992-93 Collider Run. The Collider Detector at Fermilab (CDF) was used to record these data, amounting to $\sim$19 pb^{-1} total integrated luminosity. As CDF has been described in detail previously [9], only the portions of the detector relevant to this analysis will be mentioned here. CDF consists of charged particle tracking chambers near the event vertex, surrounded by energy calorimeters and muon chambers. Charged particle tracking is obtained from the vertex chamber (VTX), and the central tracking drift chamber (CTC). These devices have approximately cylindrical geometry and are situated in a 1.4 T solenoidal magnet field, allowing high resolution transverse momentum (p_T) measurement in the pseudo-rapidity region $|\eta| <$ 1.1. Outside the tracking chambers are the electromagnetic(EM) and hadronic(HA) calorimeters, segmented in a projective tower geometry, and covering the central (CEM+CHA, $|\eta| < 1.1$) and plug (PEM+PHA, $1.1 < |\eta| < 2.4$) regions. Finally, muon identification is available in the central muon (CMU+CMP, $|\eta| < 0.6$) and muon extension (CMX, $0.6 < |\eta| < 1.1$) detectors. CDF was originally constructed with only the CMU detector; the CMP and CMX detectors were added later (providing additional hadron absorber and improved pseudo-rapidity coverage, respectively).

An initial sample of $\sim 6 \times 10^6$ events is obtained from events which have fired the CDF central electron or muon triggers (which require $p_T > 9.2$ GeV/c). We then select events containing at least one very high quality "gold" lepton (ie., that would likely have passed our trigger), and at least two additional "regular" leptons with less stringent requirements. A gold

[2]Dr. J. Wolinski is serving as co-convener of the CDF supersymmetry working group.

electron must deposit at least 11 GeV transverse energy (E_T) in the CEM, exhibit transverse and longitudinal shower profiles consistent with an electron, and be well matched to a charged track with $p_T \geq E_T/2$. A gold muon must produce a cluster in the CMU and CMP chambers, be well matched to a charged track with $p_T \geq 11$ GeV/c, and deposit calorimeter energy consistent with a minimum ionizing particle.

We now describe the various categories of regular leptons admitted in our analysis. Regular electrons are accepted in the CEM or PEM, and must have $E_T \geq 5$ GeV. In both cases, the calorimeter shower shape must be consistent with an electron, and central electrons must be well matched to a charged track with $p_T \geq E_T/2$. Since our central tracking chamber does not allow high efficiency track reconstruction into the plug calorimeter, we require a plug electron to be correlated with a high occupancy of hits in the appropriate sector of the VTX, as evidence that a charged particle produced the shower. Regular muons are muon chamber clusters in the CMU+CMP or CMX regions with $p_T \geq 4$ GeV/c, and satisfying the same muon identification criteria as those for gold muons. In addition, a charged track with $p_T \geq 10$ GeV/c is considered a muon, even without any muon chamber hits, if it deposits energy in the central calorimeters consistent with a minimum ionizing particle (this is termed a CMIO muon).

Having specified our criteria for selecting three leptons, we now turn to event quality and background rejection cuts. Since it is possible for events containing heavy flavor quarks (ie., b and c) to produce multiple leptons via semi-leptonic decay, we require each lepton to be well isolated from other particles in the event. Leptons from heavy flavor are usually embedded in jets and we thus demand that the lepton isolation, defined as the total calorimeter E_T in an $\eta - \phi$ cone of radius R = 0.4 (where R = $\sqrt{\delta\phi^2 + \delta\eta^2}$) surrounding the lepton, be < 2.0 GeV (excluding the E_T of the lepton itself). We require the longitudinal position of the reconstructed primary event vertex to lie within 60 cm of the center of the CDF. In order to remove photon conversions and pion punch-through, we require the $\eta - \phi$ distance (ΔR) between any two leptons to be greater than 0.4. Background from Drell-Yan processes is reduced by requiring the difference in azimuthal angle between the two highest p_T leptons in the event to be less than 170°. Assuming lepton number conservation, SUSY trilepton candidates must possess at least one e^+e^- or $\mu^+\mu^-$ pair. Finally, an event is rejected if it contains an $\ell^+\ell^-$ pair with invariant mass in any of the following regions : 2.9-3.3 GeV/c^2 (J/ψ), 9-11 GeV/c^2 (Υ), 75-105 GeV/c^2 (Z^0). After imposing all of these criteria, we are left with zero SUSY trilepton candidate events (see Table 1).

The efficiency with which CDF can reconstruct trilepton events consists of four principal components: geometric and kinematic acceptance, trigger efficiency, isolation efficiency, and lepton identification (ID) efficiency. We now discuss each of these entities.

The geometric and kinematic acceptance was determined via Monte Carlo simulation. ISAJET [10] was used to generate SUSY trilepton events, which were then passed through a CDF detector simulation program and the trilepton analysis code. The resulting trilepton yields give acceptances in the range of $\sim 2 - 12\%$, depending on the MSSM parameters used.

The trigger efficiency curves for single electrons and muons were obtained from CDF data samples which were not biased by the inclusive lepton triggers. These curves rise sharply around the trigger threshold of 9.2 GeV/c, and reach a plateau of 84.3±1.5%(88.6±0.7%) for muons (electrons) above 11 GeV/c. In order to properly account for the possibility that more than one lepton in a SUSY event could have fired the trigger, these trigger efficiencies were directly installed in the simulation software, providing event-by event weighting.

Table 1: Cumulative number of events left after each cut in the trilepton analysis, listed separately for the electron and muon trigger samples. The original CDF data sample corresponds to $\int \mathcal{L}dt = 19.1 \pm 0.7\ pb^{-1}$.

Cut	e triggers	μ triggers
Original sample	3,677,903	2,707,852
Dilepton events	5,472	6,606
Trilepton events	94	136
$ISO < 4$ GeV	14	33
$ISO < 2$ GeV	5	21
$\lvert z_{vertex}\rvert < 60$ cm	5	21
$\Delta R_{\ell\ell} > 0.4$	3	2
$\Delta\phi_{\ell_1\ell_2} < 170°$	2	2
$\lvert Q_1 + Q_2 + Q_3\rvert < 3$	2	2
Require e^+e^- or $\mu^+\mu^-$	2	2
Z^0 removal (75-105 GeV/c^2)	0	1
J/ψ removal (2.9-3.3 GeV/c^2)	0	1
Υ removal (9-11 GeV/c^2)	0	0

The lepton isolation efficiency was determined by studying $Z^0 \rightarrow \ell^+\ell^-$ events. One of the leptons was required to satisfy "gold" criteria. The other lepton was required to pass all "regular" lepton cuts except the isolation cut. Comparing the number of Z^0s thus selected with the number remaining after an isolation cut on the second lepton gives the single lepton isolation efficiency: 0.95 ± 0.01 for central leptons and 0.80 ± 0.03 for plug electrons. The difference between central and plug leptons is due to the larger transverse shower leakage which occurs in the plug. These isolation efficiencies were then incorporated into the Monte Carlo software.

Lepton ID efficiencies were determined by studying $Z^0 \rightarrow \ell^+\ell^-$ and $J/\Psi \rightarrow \ell^+\ell^-$ events. One of the leptons was selected with tight ID cuts; no ID criteria were imposed on the second lepton. The dilepton invariant mass was required to be consistent with the $Z^0(J/\Psi)$ mass. The event yields resulting from the cuts above were then compared with the number of events obtained after imposing gold and regular lepton ID criteria on the second lepton. The resulting lepton ID efficiencies are listed in Table 2. The values obtained from Z^0 and J/Ψ events agree well, indicating that the ID efficiencies are independent of p_T. These efficiencies were then directly installed in the simulation software.

Using the trilepton efficiency information, the expected background yield from SM processes can be estimated. These processes can be divided into two classes: direct trilepton events and dilepton plus fake lepton events. First, we discuss the trilepton category, consisting of processes which can directly produce three or more leptons in an event: WZ^0, Z^0Z^0, $t\bar{t}$, and heavy flavor production. Each of these backgrounds has been estimated by generating Monte Carlo events using ISAJET, the CDF detector simulation program, and the trilepton-event-finding code. The WZ^0 cross section was taken to be 2.5 pb and the Z^0Z^0 cross section was set to 1.0 pb [11]. For $t\bar{t}$ events, we used a top quark mass of 170 GeV/c^2 and a production cross section

Table 2: Lepton ID efficiencies obtained from $Z^0 \to \ell^+\ell^-$ and $J/\Psi \to \ell^+\ell^-$ events in CDF data. The top (bottom) portion of the table is for muons (electrons).

lepton type	Efficiency (%)
Gold CMU and CMP	89.0±2.6
Regular CMU and CMP	93.5±2.0
Regular CMX	94.0±2.9
Regular CMIO	92.5±4.2
Gold CEM	86.4±1.3
Regular CEM	89.0±1.2
Regular PEM	89.0±1.5

Table 3: Expected SUSY trilepton backgrounds in the CDF data sample (19.1 pb^{-1}), where $\ell = e, \mu$ or τ. The processes in the bottom portion of the table are multiplied by the lepton fake rate (0.28±0.02% leptons per event) to obtain a background prediction. $\sigma \cdot BR$ is the value used in Monte Carlo generation, and is quoted in picobarns.

Trilepton physics process	$\sigma \cdot BR(3\ell)$	# 3ℓ events
$WZ \to \ell\nu\ell^+\ell^-$	4.39×10^{-2}	< 0.01
$ZZ \to \ell^+\ell^-\ell^+\ell^-$	4.76×10^{-3}	< 0.01
$b\bar{b}, c\bar{c}$	–	1.15
$t\bar{t}$	7.0×BR	< 0.01
Dilepton physics process	$\sigma \cdot BR(2\ell)$	
DY $\gamma \to \ell\ell$	850.4	0.60
DY $Z^0 \to \ell\ell$	491.1	0.14
$WW \to \ell\nu\ell\nu$	0.511	< 0.01
Total		1.90

of 7.0 pb [12]. Heavy flavor production via ISAJET has one potential difficulty, the transverse energy isolation of leptons. We have investigated this by comparing heavy flavor production in ISAJET and CLEOQQ (a generator optimized for heavy flavor production [13]), and find good agreement in the lepton isolation distributions. Table 3 lists the $\sigma \cdot BR$'s (cross section · branching ratios) used in our simulations and the expected event yields in 19.1 pb^{-1}.

In the second category of backgrounds, we consider processes which can yield only two leptons: Drell-Yan, Z^0, and WW events. Such an event could pass our trilepton-finding criteria if there exists an additional fake lepton in the event. We consider a fake lepton to be an object identified as a lepton but which does not come from the main physics process (eg., misidentified jets or pions, photon conversion, decays in flight, intial state radiation producing heavy flavor quarks which decay semileptonically, etc.). We have estimated the fake rate by analysing clean $W \to \ell\nu$ and $J/\Psi \to \mu^+\mu^-$ events in CDF data. No additional isolated leptons are expected in these events (other than the leptons which reconstruct the W or J/Ψ). The results obtained

from these two samples are in agreement and have been averaged to obtain the final fake rate: 0.280±0.018% fake leptons per event. We note that since W's and J/Ψ's are produced in processes of different Q^2, we conclude that the lepton fake rate is independent of Q^2.

The lepton fake rate was then combined with Drell-Yan, Z^0, and WW events generated with ISAJET and processed in the same manner as the previous category of trilepton background events. Drell-Yan (Z^0) events were produced in the invariant mass range 15-120 (50-130) GeV/$c^2$and the production cross sections were obtained from previous CDF measurements [14, 15]. The WW production cross section was taken as 9.5 pb [11]. Table 3 lists the $\sigma\cdot$ BR values and the expected event yields in 19.1 pb^{-1}. The grand total of all expected backgrounds is 1.9 events in the CDF data sample. This is clearly consistent with our observation of zero events.

There are four primary sources of systematic error in the $\sigma\cdot$BR determined by this analysis: trigger efficiency, trilepton-finding efficiency, structure functions, and total integrated luminosity. A conservative estimate of the trigger efficiency uncertainty was obtained by assuming that all trilepton events were accepted on the single muon trigger line (as opposed to the single electron or multiple lepton lines), which has the largest efficiency uncertainty. The estimated trigger efficiency systematic error is thus $^{+2.8}_{-2.6}$%. The combined systematic error of all trilepton-finding efficiencies (kinematic, geometric, reconstruction, identification, and isolation) is $^{+14.8}_{-11.4}$%. This comes mainly from the geometric and kinematic uncertainties in the CDF detector simulation program. The CTEQ 2L structure functions [16] were used in all of our Monte Carlo studies. The SUSY trilepton production cross section and efficiency were studied by running ISAJET with various other structure functions [17] for various chargino mass values. We have used the maximum deviations from the CTEQ 2L predictions as our systematic error estimate: $^{+1.8}_{-7.6}$%. Finally, the systematic error due to the uncertainty in the total integrated luminosity is $^{+3.7}_{-3.5}$%. Combining all of these uncertainties, we obtain a total systematic error in our cross section measurement of $^{+15.6}_{-14.4}$%.

Based on our observation of zero trilepton events, we set a 95% confidence level upper limit of 3.11 events on the mean number of events expected. This result was obtained by convoluting our total systematic uncertainty of 15.6% (as a Gaussian smearing) with a Poisson distribution. This limit can then be used to exclude the particular regions of the MSSM parameter space in which:

$$\sigma \cdot BR(\tilde{\chi}_1^{\pm}\tilde{\chi}_2^0 \rightarrow 3\ell + X) \cdot \epsilon^{tot} \cdot \int \mathcal{L}dt \; > \; 3.11 \qquad (1)$$

where $\sigma \cdot BR$ is determined by ISAJET and ϵ^{tot} has been determined from efficiency studies.

Assuming SUGRA constraints which tie the slepton masses to the gluino and squark masses, the SUSY predictions from ISAJET depend on the following quantities: the pseudo-scalar Higgs mass M(H_A), the trilinear top squark coupling A_t, the ratio of Higgs vacuum expectation values $\tan\beta$, the Higgs mixing parameter μ, the gluino mass M($\tilde{g}$), and the squark/gluino mass ratio M($\tilde{q}$)/M($\tilde{g}$). The first two quantities were fixed (M(H_A) = 500 GeV/c^2, A_t = 0), since they do not significantly alter the trilepton yield. The remaining quantities do affect the predicted trilepton signal, and scanning ranges were determined as follows. ISAJET only allows $\tan\beta$ values in the range 1.0–10.0, and values close to 1.0 are theoretically disallowed ($\tilde{t}$ becomes the lightest SUSY particle). The M($\tilde{q}$)/M($\tilde{g}$) ratio is theoretically favored to be greater than unity [6] and the trilepton yield drops rapidly when this ratio exceeds 2.0 (this is due to sleptons becoming heavy, which reduces the neutralino leptonic branching ratio). Finally, our trilepton

sensitivity is lost for $|\mu|$ <100 GeV (where the gaugino masses become large, giving a tiny cross section), and $|\mu|$ is favored to be $\lesssim$1000 GeV (the approximate energy scale below which SUSY phenomena should be observable). Thus, we have scanned the following ranges of SUSY parameters: $\tan\beta$ = 2.0, 4.0, 10.0; $M(\tilde{q})/M(\tilde{g})$ = 1.0, 1.2, 2.0; 200 GeV < $|\mu|$ < 1000 GeV; $M(\tilde{g})$ = 120$\sim$250 GeV/c^2.

The total SUSY trilepton-event-finding efficiency ranges from $\sim$1-7% in this parameter region, and is approximately linearly dependent on the chargino mass. Equation 1 is then combined with the efficiency information to determine which points in the SUSY parameter space are excluded. This analysis is unable to increase the chargino mass lower limit beyond the current value (47 GeV/c^2 [18]) for any choice of SUSY parameters. However, Figure ?? shows several SUSY parameter space regions for which this analysis has increased the existing neutralino mass limit [18], reaching as high as 49 GeV/c^2. Our results can also be expressed in terms of gluino mass lower limits, but, once again, the limits set by this study are less stringent than previously existing bounds [19].

In conclusion, we have used the trilepton signature to search for $\tilde{\chi}_1^{\pm}\tilde{\chi}_2^0$ pair production in 1.8 TeV $p\bar{p}$ collisions at the Fermilab Tevatron. We find no events consistent with this process and set lower limits on the gaugino masses. The resulting chargino mass limits are less than or equal to existing bounds. However, the neutralino mass lower limits obtained are as high as 49 GeV/c^2 (depending on the region of the SUSY parameter space), substantially improving previous bounds.

Future work: We expect to submit the trilepton analysis of the Run-1A data to Phys. Rev. Lett. in January 1996.

A.2. Search for SUSY Particles in Run 1B

We have selected an inclusive dilepton event sample from the CDF exotic dilepton stream-B trigger sample, containing 3.2 million events. Those events were skimmed off, following production (Version 7.12), to 59 8-mm tapes. The events must contain at least two leptons with one lepton passing a tight cut and a second passing a loose cut. The tight-cut lepton is required to be either a central electron (CEM) or central muon (CMU/CMP). The loose-cut lepton can be a central electron (CEM), plug electron (PEM), central muon (CMU/CMP), central muon extension (CMX), or a central minimum ionizing object (CMIO) [20]. The inclusive dilepton sample contains 402 $\times$ 10^3 events and is common for the following analyses:

Chargino/neutralino: Since a degradation in the isolation cut is seen, we have selected trilepton events with a loose isolation cut (ISO < 4 GeV) and obtained 21 events. Four of them were removed because the third lepton was from the second z vertex. We are left with 17 events. Based on the analysis of Run 1A data, the most of 17 events are expected to be background. We are currently investigating additional cut to efficiently reduce the background. A detailed study is in progress.

With the Run-1B data, our reach in chargino (or neutralino) mass should be extented up to 70 GeV/c^2.

Table 4: Expected $\tilde{t}_1\bar{\tilde{t}}_1$ production cross section

$M(\tilde{t}_1)$ (GeV/c^2)	$\sigma(\tilde{t}_1\bar{\tilde{t}}_1)$ (pb)	Events in 100 pb^{-1}
70	60	6000
90	15	1500
112	4	400

Gluino/squark: A search for $\tilde{g}\tilde{g}$, $\tilde{g}\tilde{q}$, and $\tilde{q}\tilde{q}$ via a like-sign dilepton $+\not\!\!E_T$ + 2 jets signature has been suggested [21, 22, 23]. We have just submitted the analysis of the Run-1A data to Phys. Rev. Lett. [24]. The CDF mass limit at a 95% C.L. is

$$M(\tilde{g}) \;>\; 219\ (145)\ \text{GeV}/c^2 \text{ if } M(\tilde{q}) = M(\tilde{g})\ \ (M(\tilde{q}) \gg M(\tilde{g})),$$

which is comparable to the limit set by a classical $\not\!\!E_T$+ Multijet analysis [19].

The analysis of the Run-1B is in progress: we are reducing the size of the initial dilepton sample (402×10^3 events) by requiring additional two (or more) jets with a missing transverse energy. We expect a preliminary result in spring, 1996.

Top-squark: In addition, we search for a light top squark ('stop' or $\tilde{t}_1$) in a dilepton mode. Table 4 shows the expected production cross section of $\tilde{t}_1\bar{\tilde{t}}_1$. The decay mode of $p\bar{p} \to \ell\ell + b\bar{b} + \not\!\!E_T$ is similar to the SM $t\bar{t}$ decay. However, the transverse momenta of leptons and jets are expected to be smaller. Therefore, we distingush the signal events from background by requiring $B = |p_T(\ell^+)| + |p_T(\ell^-)| + \not\!\!E_T < 100$ GeV [25]. Currently, we try to understand the background.

With an integrated luminosity of 100 pb^{-1}, we should be able to probe top squark masses up to 70 GeV/c^2 [25].

B. CDF Operation

The most important job for the CDF collaboration in Run 1B (1994-1995) was to take data at high efficiency. With 'ACE' and 'Operation Help' systems, the CDF 'data-on-tape' efficiency was near 75% in Run 1B. The ACE is a person who runs the CDF on-line data acquisition system (hardware & software) during runs. During Run 1B we provided two 'ACE' persons and one 'operation help' person. Mr. Tannenbaum served as ACE from the Texas A&M group.

The high data-taking efficiency was also due to the effort of each subdetector group. Our group contributed maintenance of the forward hadron calorimeter (FHA) system.

Summary of FHA performance in Run 1B Operation of the forward hadron calorimeter (FHA) during the Tevatron collider Run 1B was typically fairly smooth. The total downtime of the data taking due to the FHA system was less than 0.1%.

The most bothersome problem which occurred occasionally during the run was the development of high voltage shorts in individual FHA layers. At the beginning of Run 1B, only 4 FHA chambers were unusable.[3] During Run 1B, additional 11 FHA layers were lost in 21 months, requiring correction factors between 0 and 6%. Since there are over 200 layers in the FHA detector system, this is not an unduly large fraction. Furthermore, not all of these layers were disabled throughout the run, since it is possible to partially recover a shorted layer during a CDF collision hall access. Indeed, 6 layers were resuscitated during the run by isolating the smaller region of the layer that actually contained the short.

It should be noted that no significant trigger rate change was observed during the run that can be associated with dead FHA layers.

Another problem which occurred during a particular brief period of Run 1A was the appearance of excessive noise in one of the FHA quadrants. We identified the source of this problem to be a faulty printed circuit board that has existed in the FHA calorimeter since it's construction. The circuit board flaw was repaired during the long access between Run 1A and 1B. The noise problem has not reocurred.

FHA for Run 1C: The FHA system and its monitoring softwares are ready for Run 1C. DB_ANA (a set of CDF database analysis tools) is helpful in displaying any vital electronics information. FHAMON (FHA diagnostic) and YMON (CDF monitoring software) can assist us to locate any problem that can arise with the FHA. HVMON (high voltage software) allows us to regulate and monitor the current that is delivered to the FHA. Oxygen analyzers, pressure indicators and GASDAQ (Gas Data Aquisition System) allow us to monitor the quality of the gas that is used in the calorimeter.

Future work: Run 1C started in November 1995, and will end in February, 1996. We continue to support the smooth data taking: Dr. Wolinski, Mr. J.P. Done, and Mr. B. Tannenbaum are regularly monitoring the FHA data quality and will provide the FHA energy scale for the Run 1C data.

[3]Two of these are relatively unimportant, due to their position at the very end of the hadronic shower. The other two layers were found to be stuck in the absorber steel and thus could not be accessed for repair without destruction of the FHA.

C. CDF SVX-II[4]

C.1. Radiation Hardness Testing of Optical Fibers[5]

Introduction: The current design of the SVX-II detector requires it to be read out at a rate of at least 53 Mbytes/second using electrical signals. These signals would travel on a short (few inches) transmission line to a port card mounted at the outer radius of SVX-II. The port card converts these electrical signals into optical signals. Optical fibers will then take the data (at 53 Mbytes/second) to a "Glink" board housed in a crate mounted on the face of the CDF central detector. For approximately 1 meter, the optical fiber will be in a high radiation environment and will receive a lifetime dose of no more than 100 kRad. As radiation-hard optical fiber is both difficult to obtain and expensive, we have explored the option of using a non-radiation hard fiber [26].

Testing procedures and results: For this test, the DAQ group purchased 80 meters of AT&T ribbon cable (12 62.5μm fibers) fitted with MAC II optical connectors. We had hoped to characterize the fiber using 1300 nm and 1550 nm diode lasers. However, the cost of these lasers is quite high and instead we used 850 nm and 1300 nm LEDs (See Table 5 for LED properties). We pulsed the LEDs with a 10 MHz square wave. The light from the LEDs went through the fiber and into Tektronic optical/electrical converters (Tektronic P6701A for the 850 nm LED and Tektronic P6703A for the 1300 nm LED). The output from the converters was fed into an oscilloscope and we measured the peak to peak voltage (V_{pp}, in mV) of the resulting output wave as a function of the dose delivered. We also measured the speed of light through the fiber. Finally, we examined the physical properties of the fiber to ensure that it was physically able to withstand the required dose without becoming brittle or otherwise less robust.

Table 5: Properties of LEDs used in this test.

	OPTEK OPF372A 850 nm LED	Hewlett Packard HFBR-1312T 1300 nm LED
Input Current (mA)	100	100
Driving Voltage (V)	1.7	1.4
Output Power (μW)	89	20
Rise Time (ns)	6.0	1.8

To perform the test, 2.5 meters of the fiber was wrapped around a G10 board and placed in the 1b beamline of the 500 MeV proton source at TRIUMF in Vancouver, British Columbia.

[4]Texas A&M group is working for Monte Carlo and DAQ subgroups in the SVX-II project. Texas A&M members: T. Kamon, J.P. Done, B. Tannenbaum and J. Wolinski. Dr. Kamon is the convener of the MC subgroup.

[5]The measurement was completed in 1994. However, the calibration of the radiation monitor has been completed recently. Therefore, we revised the original report.

The fiber was wrapped in a 2 cm radius circle (well above the 1 cm bending radius of the fiber) and the light through the fiber was monitored from a counting room. Figure 4 shows the experimental setup. Between 8 September and 11 September 1994, the fiber was irradiated. Our initial calibrations led us to believe the fiber had received a total dose of approximately 1 MRad, the desired amount. We calculated a conversion factor of 1 Mrad = 3×10^{13} protons/cm^2 = 135×10^6 polarimeter counts. The polarimeter was in front of the first board; our board was in slot 20 and a rough estimate places our dosage at 60% of that delivered to the front of the stack. We had three methods of measuring dose/time– the polarimeter, two ion chambers placed before and after the stack of boards, and two PIN silicon photodiodes placed in similar positions.

After our equipment was returned to Fermilab, the Fermilab ES&H Section Activation Analysis Laboratory began to measure the small aluminum foils we placed on each board to measure total dose. This took some time and was only recently completed. The total dose the cable received was 200 $\pm$ 20 kRad as determined from AL foil counting for the reaction $p^+ + Al \longrightarrow^{27} Na + X$.

Three redundant methods for online monitoring of fluence failed during the run. (These were the 1b beamline polarimeter, two ion chambers and two PIN silicon photodiodes.) Thus no accurate record remains of the transmission versus delivered dose. Instead, a plot of transmission versus time for the first day of running, when the delivery rate was relatively constant, is presented in Figure 5. As can be seen, the fiber saturates at something less than the total dose of 200 kRad and receives relatively little damage after that point. Also, the transmission of light through the damaged fiber is a function of wavelength– the longer the wavelength, the better the transmission.

After the fiber returned from Canada (a delay of six weeks), it was re-tested by again pulsing the fiber at 10 MHz. No "recovery" was observed; the transmission was identical to the last measurement taken at TRIUMF. The physical flexibility and integrity of the fiber-optic cable was unchanged as a result of exposure.

Conclusion: While this particular fiber will not be used,[6] we believe our results apply to non-radiation hard glass core fiber in general. Based on the available data, this type fiber is indeed acceptable for our purposes. The lasers currently being developed by our Taiwanese collaborators and those available commercially are significantly more powerful than the LEDs used in this test. Also, the physical properties of the fiber were not dramatically altered. Thus, by using these powerful lasers and sufficiently sensitive receivers, a fiber of this type should last the lifetime of the SVX-II detector.

C.2. Radiation Hardness Testing of ACTEL FPGAs

Introduction: The current CDF silicon vertex detector, SVX′, is an excellent device and has greatly assisted CDF in its search for the top quark and in many other aspects of analysis. However, it will not function adequately for Fermilab's Run II. During Run II the number of p and $\bar{p}$ bunches will be increased from 6 each to 36 each, resulting in a much shorter bunch spacing of 132 ns. This requires a read-out speed far beyond the ability of the current device.

[6]This fiber has a jacket that is far too large to permit all the necessary fiber to fit in the allowed space.

To maintain (and increase) the functionality of the CDF detector, a new silicon vertex detector (SVX-II) has been designed. This new device will have an appropriate read-out speed and will have r-ϕ resolution of $\approx 10\mu$m. It will also be able to measure the z position of a track and will have r-z resolution of $\approx 25\mu$m [26].

We are presently specifying and designing the data acquisition system for this new detector. This data acquisition system requires a module, called the port card, which sits very close to the front-end electronics and controls the radiation-hard custom designed SVX chips. The SVX chips interface and read out the silicon detectors. One approach to implement the controller for the SVX chips is to add a Field Programmable Gate Array (FPGA) to the port card. However, during the run, the entire detector, including the port card and these FPGAs, will be bombarded with radiation, damaging all parts to different degrees. Therefore, the FPGAs have to be radiation-resistant, to a estimated dose of about 100 KRads over the 3 year lifetime of the detector [26]. Radiation-hard FPGAs are becoming available on the market, but they cost from $6000 to $9000 each, depending on the complexity of the part. To reduce cost, we have tested non-radiation-hard commercial grade FPGAs, to determine if they are radiation resistant enough to be used in our detector.

There are several commercial grade FPGAs available on the market and the literature reports several radiation hardness tests done with these parts [27, 28, 29, 30, 31]. However, all of these tests involve gamma radiation. In the SVX-II, the major source of damage will be high energy protons. Even so, these tests allowed us to *a priori* select certain types of FPGAs which have a good chance of withstanding the radiation type and dose we will encounter in the SVX-II detector. These previous studies caused us to select the Actel parts [32].

Testing procedures: For this test, Actel donated twenty FPGAs, of two different types (A1020B and A1240). Each set of ten chips came from one of two lots (for four total lots). Figure 6 shows the block diagram of the circuit programmed inside the Actel parts. It is a toggle flip-flop which feeds a shift register. The shift register is as deep as the part allows. This resulted in the use of 80-90% of all resources inside the A1020B part, and 80-90% of all flip-flops in the A1240 part. We monitored the clock input of the circuit, as well as the output of the shift register. We powered each FPGA with +5V DC and measured the current. We also pulsed the circuit with 5, 10, and 20 MHz signals and recorded the output.

We irradiated a total of 16 chips at the 4B beamline of the 500 MeV proton source at TRIUMF in Vancouver, British Columbia in April, 1995. We tested two chips of each type and lot to two different integrated doses (100 kRad and 250 kRad).

To perform the test, we mounted each chip in a socket attached to a breadboard and placed them in a beam box. This box held the breadboards perpendicular to the proton beam. During the test the FPGAs were held at a constant 17° Celsius. The chips received +5 volts DC, and we recorded the current as a function of integrated dose. Any chip that drew more than 150 mA was disconnected from the power supply and received the remainder of the dose unpowered. Each chip had a small (1 cm × 1 cm) piece of aluminum foil taped to the front surface. The radiation activated the foil, and by measuring the Na^{22} line we can determine the actual dose received by the chip.

We removed chips from the beam box when our online fluence monitor, a polarimeter, indicated they had received the desired dose. The polarimeter was calibrated to reflect the dose

Table 6: List of the desired, expected, and actual integrated dose for each chip. All doses are in kRad. Note that the actual dose is 40-60% of the measured dose. This is because the chips were placed towards the rear of the beam box and the online fluence measurement was calibrated for cards in the front of the box.

Chip Type	Lot	Chip ID	Desired Dose	Calculated Dose	Measured Dose
			(kRad)		
A1020B	1	1	100	87	40
A1020B	1	2	100	87	40
A1020B	1	3	250	284	130
A1020B	1	4	250	284	120
A1020B	2	1	100	129	70
A1020B	2	2	100	129	70
A1020B	2	3	250	299	120
A1020B	2	4	250	299	130
A1240	1	1	100	87	30
A1240	1	2	100	129	70
A1240	1	3	250	284	110
A1240	1	4	250	299	120
A1240	2	1	100	129	60
A1240	2	2	100	129	60
A1240	2	3	250	299	120
A1240	2	4	250	299	110

received by the board in the front of the beam box. Our materials were in slots 21 through 25 and received a somewhat smaller dose.

Results: After our equipment was returned to Fermilab, the Fermilab ES&H Section Activation Analysis Laboratory began to measure the aluminum foils we placed on each board to measure total dose. The analysis of the foils was completed by the Radiation Metrology Laboratory at Sandia National Laboratories. This measurement was only recently completed. The total dose received was determined from Al foil counting for the reaction $p^+ + Al^{27} \longrightarrow Na^{22} + X$. Table 6 lists the desired, online-measured, and actual dose each chip received.

After the parts were returned to Fermilab, we tested the parts again to determine if they had survived the dosing. To perform this test, we first applied +5V DC to each chip and measured the current. Next, we applied a 20 MHz clock signal and again measured the current draw. Finally, we removed the clock signal and measured the current again. Tables 7 and 8 show these results. All of the Actel 1020B devices survived the radiation damage, while none of the Actel 1240 survived . The 1240 has a higher circuit density and we believe this makes it more susceptible to radiation damage.

Table 7: Current drawn by the Actel 1020B before and after radiation for a DC input and a 20 MHz clock. The entries marked with a question mark gave unusually low readings after the chips were dosed. Those marked with an asterisk failed to return to the lower current draw when the clock signal was removed. However, when the power was removed and restored, they did return to the lower current draw.

Actel 1020B

	I_{cc} (mA) for +5V DC							
	Lot 1				Lot 2			
	100 kRads		250 kRads		100 kRads		250 kRads	
Before radiation	0.74	0.71	0.71	0.72	0.76	0.71	0.76	0.76
After radiation	22.9	23.0	1.0?	1.0?	39.6	37.7	39.1	38.5
	I_{cc} (mA) for +5V DC and 20 MHz clock							
Before radiation	146	146	145	145	144	144	146	147
After radiation	173*	165	149	128	221	219	228*	218*

Table 8: Current drawn by the Actel 1240 before and after radiation for a DC input. None of the chips would function when a 20 mHz clock signal was applied, implying all eight chips were disabled by the exposure. The entries marked with a question mark gave unusually low readings after the chips were dosed.

Actel 1240

	I_{cc} (mA) for +5V DC							
	Lot 1				Lot 2			
	100 kRads		250 kRads		100 kRads		250 kRads	
Before radiation	0.22	0.51	0.21	0.20	0.20	0.19	0.20	0.20
After radiation	137	1.2?	3.3?	221	220	232	197	199

Conclusions: Based on the available data, we believe the Actel FPGA 1020B (or a similar part) is acceptable for our purposes. All eight chips survived the radiation damage with minimal change in function. Four chips survived a total integrated dose of greater than 100 kRads, comparable to the lifetime dose expected at the port card. While we do have data for current draw as a function of dose, we are hesitant to extrapolate our results to higher integrated doses as the instantaneous current draw was a function of both the beam current and the current drawn by the chip. Due to the results obtained in these tests, we believe the Actel 1020B is sufficiently robust to last the lifetime of the SVX-II detector.

Future work: We, within the DAQ group, continue working on optical fiber quality control, the detector readout system and supply of electrical power to the detector. In conjuction with the MC occupancy study, we are pursuing more accurate estimate of the DAQ deadtime.

C.3. SVX II z-vertexing Study Using CDFSIM

We have evaluated two SVX-II design options using CDFSIM and GEANT3 [33]. The results are summarized below:

- Four-layer option: The optimal readout configuration in z is the 4-3-3-2 scheme for four 90° stereo layers and the detector is capable of self-vertexing in z with a resolution of about 200 μm for MB events and 60 μm for $t\bar{t}$ events;
- Five-layer option: The optimal readout configuration in z is listed by layer(angle): 0(90°)-1(90°)-2(+1°)-3(90°)-4(−1°).

The CDF collaboration decided to build five-layer SVX-II system.

The algorithm of the self-vertexing in z was developed using GEANT3 [34]. We are converting the GEANT3 code to CDFSIM code and testing it. The algorithm of our method is outlined below:

- Find the charge weighted centroids of the clusters [36];
- Intersect the r-ϕ and stereo r-z clusters [35];
- Draw line segment formed from two 90° layer cluster positions;
- Trace segment through layers;
- Minimize the χ^2_{fit};
- Look at 4 and 5 hit tracks;
- Trace line to beam pipe to find z-vertex of the track;
- Write out VTVZ bank.

In a preliminary study, the CDFSIM code finds the z vertex with a resolution of approximately 200μm [37].

Future work: We need to refine our algorithm to take into account multiple primary vertices that will be created in Run II's luminosity regime.

D. Tevatron Physics Beyond the Main Injector

TeV2000 group was formed at the first meeting at the University of Michigan (October 21-22, 1994) to organize the physics working groups (top, electroweak, low-mass Higgs, low-energy SUSY, and exotics) at a luminosity upgraded Tevatron (called TeV33) beyond the Main Injector. Dr. T. Kamon is serving as co-conviner (with Dr. K. De, Univ. of Texas at Arlington) of "Low-energy SUSY" working subgroup. The purpose of our effort is to indentify the physics which can be done competitively even in the LHC era. We listed several milestones of our effort:

10/21/94	First TeV2000 group meeting, University of Michigan.
11/11/94	SUSY group meeting, Fermilab.
12/ 6/94	SUSY group meeting, Texas A&M University.
12/15/94	TeV2000 organization meeting, Fermilab.
4/ 7/95	TeV2000 group meeting, Fermilab.
6/15/95	Draft report submitted to the Fermilab PAC.
12/ 8/95	Review of SUSY report by TeV33 Review Committee (chaired by Dr. Bardeen), Fermilab.

Below is an exective summary of SUSY report to TeV33 Review Committee (December 14, 1995):

SUSY Summary Report to TeV33 Review Committee

(December 14, 1995)

The Standard Model (SM) of particle physics is in remarkably excellent agreement with existing data. In spite of this fact, there are strong theoretical arguments to suggest that the SM will break down in the TeV domain. Thus high energy physics is currently in the unique position of having a theory that works at a level of high precision, but must in fact be modified at an energy scale not far above existing accelerators. There are of course many reasons for building a new high energy accelerator. However, in view of the present status of high energy physics, a primary purpose must be to discover new physics.

Any model of new physics must face the difficult task of accommodating the high precision tests of the SM, and yet significantly modifying it at an energy scale not much beyond the Z boson. Further, the solution that supersymmetry (SUSY) gives to the hierarchy problem requires that there be a large array of new SUSY particles lying approximately between 100 GeV and 1 TeV. In spite of this, supersymmetry succeeds in perturbing the successes of the SM negligibly due to the fact that it implies the rapid decoupling of these particles from the SM particles. Further, experimental searches for the SUSY particles have examined only a very small part of the expected mass range of 100 GeV - 1 TeV, and so it is not surprising that the new SUSY particles have not yet been discovered. It is thus of importance for new accelerators to try to increase the mass reach if supersymmetry is to be tested.

The SUSY model the TeV33 SUSY group analysed was based on the particle spectrum of the MSSM (a SUSY partner for each SM particle with two Higgs doublets) combined with grand

unification (based on supergravity) and R parity. (Supergravity is the gauge theory of global supersymmetry (MSSM) just as Yang-Mills theory is the gauge theory of global (constant) phase invariance.) This model is the most attractive from both the theoretical and experimental considerations. The supergravity induced interactions allow one to deduce the soft breaking of supersymmetry at the GUT scale (which only can be done by hand for the low energy MSSM), and from this one obtains an explanation of the origin of electroweak symmetry breaking at the Z scale by radiative effects. In addition, low energy predictions are almost all independent of the grand unification group, and hence of the unknown GUT physics. Several experimental successes have led to the acceptance of the model. It predicted the existence of grand unification more than a decade before the precision LEP data allowed its verification. Further, unification occurs if SUSY masses are precisely in the range needed to resolve the gauge hierarchy problem mentioned above. The model is also consistent with the low energy SM tests, as well as current bounds on proton decay. Finally, we mention that the condition of R parity invariance leads to a stable lightest supersymmetric particle (LSP) which gives the right amount of dark matter over a large fraction of the parameter space. (This prediction is non-trivial as the relic dark matter density depends on such disparate quantities as the electroweak coupling constant,the LSP mass, the gravitational constant and the Hubble constant.)

If one adds additional light Higgs doublets to the particle spectrum, agreement with grand unification (or proton decay bounds) is lost, while a Higgs singlet would generally destabilize the gauge hierarchy. While the assumption of four generations (though not more) is still consistent with grand unification, it would ruin the prediction of m_b/m_τ for groups such as SU(5) or SO(10). Thus, the chosen model is fairly constrained, and it is therefore worthwhile to use it as the prototype for accelerator tests.

The minimal version of this SUSY model (MSGM) depends on four parameters and one sign to describe the masses and interactions of the 32 new SUSY particles: m_0 (universal scalar mass), $m_{1/2}$ (universal gaugino mass), A_0 (cubic soft breaking term), $\tan\beta$, and the sign of μ (the Higgs mixing parameter). For simple GUT groups, it is difficult to construct a theory where universality of $m_{1/2}$ is lost by more than about 10%. Any non-universality in m_0 or A_0 will not affect any of the experimental signals available to the TeV33 discussed in the SUSY section. Therefore, the MSGM is the best representative model to study SUSY physics.

A model with so few parameters allows a number of predictions of the mass spectrum. Thus there are a number of light particles present, *e.g.*, the light Higgs (h) has a mass bound $m_h \lesssim$ 130 GeV ($m_h \lesssim$ 150 GeV for a theory with arbitrary Higgs content). The theory also predicts the existence of a light chargino ($\tilde{\chi}_1^\pm$) and two light neutralinos ($\tilde{\chi}_{1,2}^0$). These are generally lighter than the gluino and hence most accessible to observation. For example, for $\mu^2 \gg m_Z^2$ (*i.e.*, $\mu \gtrsim 3m_Z$) one has $m_{\tilde{\chi}_1^\pm} \simeq m_{\tilde{\chi}_2^0} \simeq 2\, m_{\tilde{\chi}_1^0} \simeq (\frac{1}{3} \sim \frac{1}{4}) m_{\tilde{g}}$. The $m_{\tilde{\chi}_1^0}$ is the LSP for almost the entire parameter space.

The SUSY mass limits at TeV33 (25 fb^{-1}) are compared to the limits expected at LEP-II and NLC in Table 9 [38, 39]. While LEP-II can find or exclude the light chargino ($\tilde{\chi}_1^\pm$) and light top-squark ($\tilde{t}_1$) masses up to nearly its kinematical limit ($\sqrt{s}/2$), searches at TeV33 improve a reach 2-3 times that of LEP-II. If LEP-II found a 90-GeV chargino, we should study 270-360 GeV gluino at TeV33. A preliminary study on determination of gluino mass shows the 300-GeV gluino mass could be measured within about 20 GeV [41]. TeV33 is also competitive to NLC in the gluino/squark searches. Thus, the SUSY searches at TeV33 is complementary to those at LEP-II and NLC.

We recommend that Fermilab should make a coherent effort to deliver an integrated luminosity of order 20-25 fb^{-1} (not 100 fb^{-1}) with reasonably upgraded CDF and D0 detectors, so that we can have the first physics result within ~1 year after LHC turns on. If the gluino (chargino) is $\leq$ 400 (250) GeV, TeV33 still has a chance to discover the SUSY particles during the LHC era. It should be noted that the light Higgs (h) search is also an important concomitant search, since SUSY predicts it to be lighter than 150 GeV.

Table 9: Summary of SUSY mass limits at various colliders. "Exhaustive limit" means the least mass limit. Searches at LHC are not shown here. However, the limits are largely improved, *e.g.*, 1300-2000 TeV for gluino depending on the choice of the parameter space.

Collider	LEP-II [38]	TeV33 [39]		NLC [38]
$\sqrt{s}$	190 GeV	2 TeV		500 GeV
$\int \mathcal{L}dt$	500 pb^{-1}	25 fb^{-1}		20 fb^{-1}
	Max. limit	Exhaustive limit	Max. limit	Max. limit
$\tilde{\chi}_1^{\pm}$	90 GeV	65 GeV [40]	250 GeV	248 GeV
$\tilde{g}/\tilde{q}$	85 GeV (100 pb^{-1})	275 GeV	over 400 GeV	~250 GeV
$\tilde{t}_1$ ($\rightarrow c\chi_1^0$)	83 GeV	45 GeV (2 fb^{-1})	120 GeV (2 fb^{-1})	~250 GeV
$\tilde{t}_1$ ($\rightarrow b\chi_1^{\pm}$)	N/A	150 GeV	180 GeV	~250 GeV

E. Proposed Research in the Next Funding Year

It is clear that the physics and detector R&D programs in CDF experiment remain very exciting research projects:

- Supporting the Run 1C operation (1995-1996) to provide the best gas calorimeter energy scale for the top, W, SUSY, and other physics analyses with the $\not\!\!E_T$ signature;
- SVX-II project (1996-1998) for Run II (in 1999);
- Physics analyses (1996-1998).

The current members are T. Kamon, P. McIntyre, R. Webb (Faculty); J. Wolinski (Assistant Research Scientist); J.P. Done, J. Lu, B. Tannenbaum (Graduate Students).

With about 100 pb^{-1} data collected with CDF in Run 1A and 1B, we should be able to test a new physics beyond the Standard Model: supersymmetry. Our group will lead CDF's SUSY searches for $\tilde{\chi}_1^{\pm}$, $\tilde{g}/\tilde{q}$, and $\tilde{t}_1$ particles.

The upgraded Silicon Vertex detector (SVX-II) should be installed in 1998 for Run II expected with the Fermilab main injector in 1999. We will work on (a) the evaluation of physics performance, (b) the simulation and analyses packages, (c) DAQ optical fiber readout system and (d) the installation and commissioning of the SVX-II detector. The SVX-II MC group is also working with the CDF Tracking Upgrade group to pursue the design.

We keep developing an idea of possible luminosity upgrade to the Fermilab Tevatron complex, beyond construction of the Main Injector. In order to identify the physics program even in the LHC era, it is very important to study a degradation of the physics performance at TeV33. Only TeV2000 SUSY group provided preliminary results on the lepton isolation and missing transverse energy. This work should be continued by extending our effort in respect to the current CDF physics analyses.

In summary, our research will be focused on the CDF experiment and its related future project (physics with an upgraded CDF detector). We list our personnel for this research proposal in Table 10.

Table 10: Summary of Texas A&M personnel and research time for the CDF experiment.

Name	< %CDF >	Operation	Physics	SVX-II
T.Kamon	100	5	50	45
P.McIntyre	25	5	20	0
R.Webb	25	5	20	0
J.Done	100	10	50	45
B.Tannenbaum	100	5	50	45

References

[1] L.Susskind, Phys. Rev. **D20**, 2619 (1979).

[2] U.Amaldi, W.de Boer, and H.Furstenau, Phys. Lett. **B260**, 447 (1991); P.Langacker and M.-X.Luo, Phys. Rev. **D44**, 817 (1991).

[3] Y.Golfand and E.Likhtman, JETP Lett. **13**, 323 (1971); J.Wess and B.Zumino, Nucl. Phys. **B70**, 39 (1974).

[4] H.P.Nilles, Phys. Rep. **110**, 1 (1984); H.E.Haber and G.L.Kane, Phys. Rep. **117**, 75 (1985).

[5] P. Nath and R. Arnowitt, Mod. Phys. Lett. **A2**, 331 (1987); R. Barbieri, F. Caravaglios, M. Frigeni and M. Mangano, Nucl. Phys. **B367**, 28 (1991); H. Baer and X. Tata, Phys. Rev. **D47**, 2739 (1992); J.L. Lopez, D.V. Nanopoulos, X. Wang and A. Zichichi, Phys. Rev. **D48**, 2062 (1993); H. Baer and X. Tata, Phys. Rev. **D48**, 5175 (1993).

[6] L.E.Ibanez, C.Lopez, and C.Muonz, Nucl. Phys. **B256**, 218 (1985); M.Drees and M.Nojiri, Nucl. Phys. **B369**, 54 (1992).

[7] For a recent review, see R. Arnowitt and P. Nath, "Supersymmetry and Supergravity: Phenomenology and Grand Unification," Proceedings of VIIth J.A. Swieca Summer School, Campos do Jordao, Brazil, 1993 (World Scientific, Singapore, 1994).

[8] P.Langacker, Phys. Rep. **72**, 185 (1981).

[9] F.Abe *et al.*, Nucl. Instrum. Methods Phys. Res., Sect. A **271**, 387 (1988).

[10] H. Baer, F.E. Paige, S.D. Protopopescu and X. Tata, "Simulating Supersymmetry with ISAJET 7.0/ISASUSY 1.0," Proceedings of Workshop on Physics at Current Accelerators and the Supercollider, eds. J. Hewett, A. White and D. Zeppenfeld (Argonne National Laboratory, 1993); F.E. Paige and S.D. Protopopescu, "ISAJET: A Monte Carlo Event Generator for pp and $p\bar{p}$ Reactions," Brookhaven National Laboratory Report No. BNL-38774 (1986), (unpublished).

[11] K.Hagiwara, J.Woodside, and D.Zeppenfeld, Phys. Rev. **D41**, 2113 (1990); J.Ohnemus, Phys. Rev. **D44**, 1403 (1991); J.Ohnemus, Phys. Rev. **D44**, 3477 (1991); J.Ohnemus and J.F.Owens, Phys. Rev. **D43**, 3626 (1991).

[12] CDF Collaboration, Phys. Rev. Lett. **74**, 2626 (1995).

[13] P.Avery, K.Read, and G.Trahern, "QQ: A Monte Carlo Generator," CLEO Software Note CSN-212, March 25, 1985.

[14] F.Abe *et al.*, Phys. Rev. **D52**, 2624 (1995).

[15] F.Abe *et al.*, Phys. Rev. Lett. **67**, 2418 (1991).

[16] H.L.Lai *et al.*, Phys. Rev. **D51**, 4763 (1995).

[17] For a summary of available structure functions, see H. Plothow-Besch, Comput. Phys. Commun. **75**, 396-416 (1993).

[18] ALEPH Collaboration, Phys. Lett. **B244**, 541 (1990) and Phys. Rep. **216C**, 253 (1992); DELPHI Collaboration, Phys. Lett. **B247**, 157 (1990); L3 Collaboration, Phys. Lett. **B233**, 530 (1989) and Phys. Rep. **236**, 1 (1993); OPAL Collaboration, Phys. Lett. **B240**, 261 (1990) and Phys. Lett. **B248**, 211 (1990).

[19] J. Hauser, The CDF Collaboration, FERMILAB-CONF-95/172-E. Published Proceedings 10th Topical Workshop on Proton-Antiproton Collider Physics, Fermi National Accelerator Laboratory, Batavia, IL, May 9-13, 1995.

[20] J. Done, "SUSY Dilepton Selection for Run 1B," presented at CDF Exotics Meeting, November 1995.

[21] R. M. Barnett, "Measuring the Gluino Mass Using Like-Sign Dileptons," Properties of SUSY Particles Proceedings of the 23rd Workshop of the INFN Eloisatron Project October 1992.

[22] H. E. Haber, "Phenomenology of Gluino Searches at the Tevatron," International Workshop on Supersymmetry and Unification of Fundamental Interactions SUSY'93, March 1993.

[23] H. Baer *et al.*, Phys. Rev. D36, 96 (1987).

[24] F. Abe *et al.*, "Search for Gluino and Squark Cascade Decays at the Fermilab Tevatron Collider," submitted to Phys. Rev. Lett (1995).

[25] H. Baer, J. Sender and X. Tata, "The Search for Top Squarks at the Fermilab Tevatron Collider," FSU-HEP-940430 and UH-511-788-94 (1994).

[26] N. Bacchetta, *et al.* "SVX II Upgrade Proposal & Simulation Study," CDF Note 1922, (January 1993).

[27] G.K. Lum, R.J. May and L.E. Robinette, "Total dose hardness of field programmable gate arrays," IEEE Trans. Nuclear Science, vol. 41, no. 6 pp. 2487-2493, Dec. 1994.

[28] W. Vaughan, "Xilinx XC3090-70 single event upset and single event latch-up test results," Internal Report No. HRTR-TM-154, Xilinx, July 1992.

[29] W. Vaughan, "Gamma radiation total dose tolerance. Testing plan for Xilinx XC3090 programmable gate array, rev A," Internal Report HRTR-TM-062, Xilinx, Feb. 1991.

[30] Altera, "Total-dose radiation hardness of Altera EPLDs," Application Brief 51, ver. 3, Sept. 1991.

[31] JPL database

[32] Actel data book.

[33] J. Antos *et al.*, "SVX-II 5th Layer Design," CDF Note 2870 (1995).

[34] J. Done *et al.*, "A Study of the z-vertexing Performance of the SVX-II (Barrel) Using GEANT3," CDF Note 2170 (1993).

[35] H.-Y. Chao, "Intersection of r-ϕ and r-z clusters," private communication.

[36] J. Antos and H.-Y. Chao, "Clustering and Track Reconstruction Package for SVX II," CDF Note 2384 (1994).

[37] J. Done and T. Kamon, "SVX II z-vertexing Simulation Study Using CDFSIM," presented in the CDF SVX II Meeting (1995).

[38] H. Baer *et al.*, "Low Energy Supersymmetry Phenomenology," DPF Report (FSU-HEP-950401, LBL-37016, UH-511-822-95) (1995).

[39] TeV2000 SUSY Group, "SUSY Physics," TeV2000 Report (1995).

[40] LEP experiments announced new results at $\sqrt{s} = 140$ GeV on December 12, 1995. The new limit on $\tilde{\chi}_1^{\pm}$ is about 65 GeV.

[41] S. Mrenna, private communication.

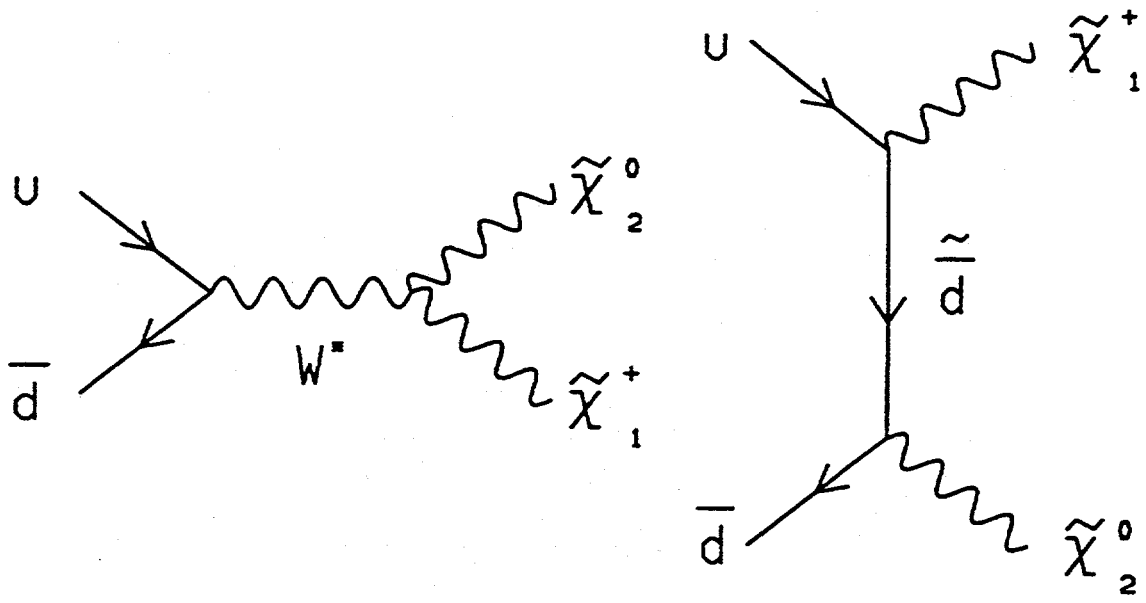

Figure 1: Feynman diagram of chargino-neutralino production.

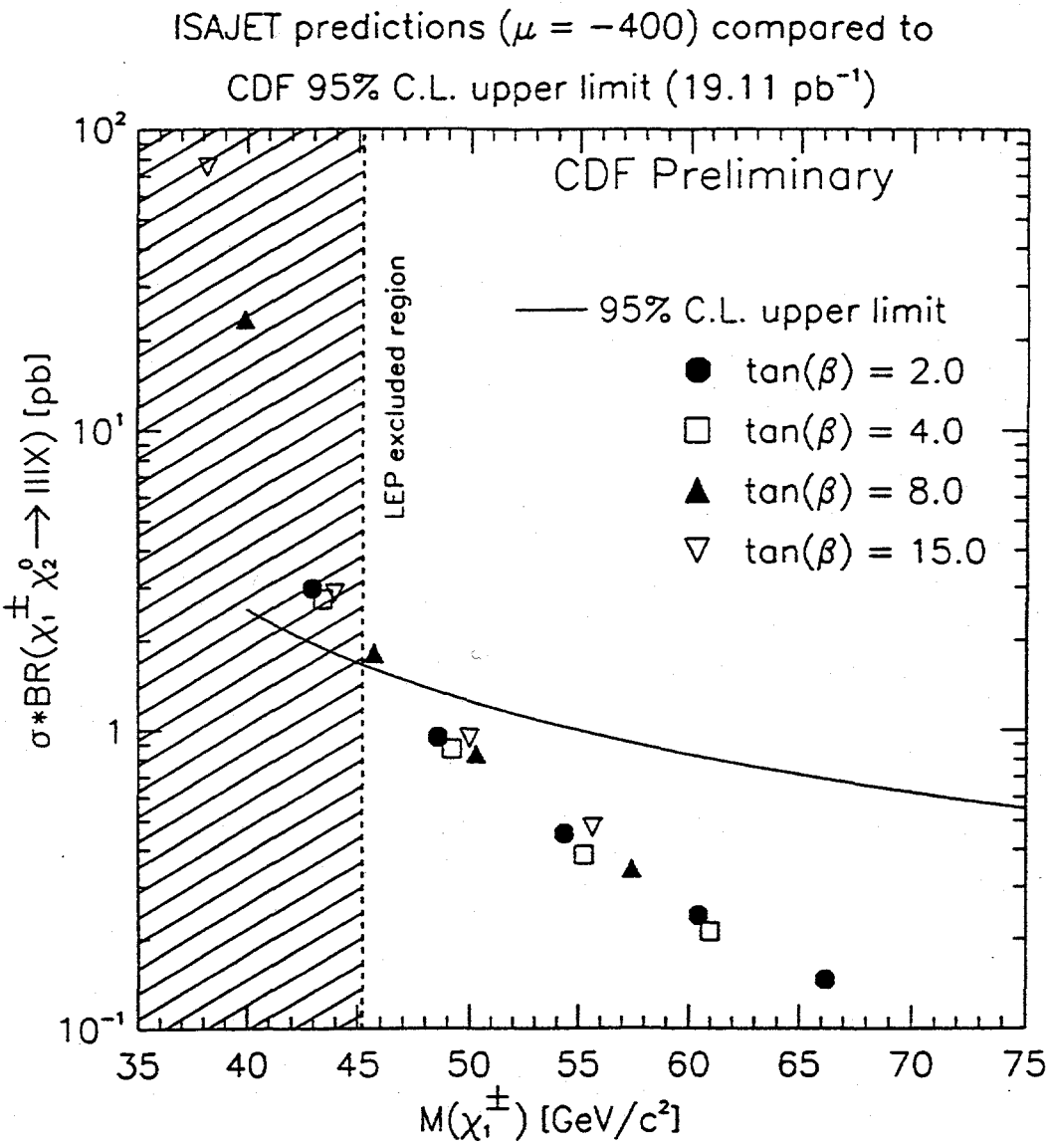

Figure 2: 95% confidence level upper limit on $\sigma \cdot BR(\tilde{\chi}_1^{\pm}\tilde{\chi}_2^0 \rightarrow 3\ell X)$ vs. $M(\tilde{\chi}_1^{\pm})$. The data points are the predictions of ISAJET 7.06. Note that 3ℓ does NOT refer to the sum of all four modes, but rather any one of them individually (ex., eee). The shaded region corresponds to the LEP limit [18].

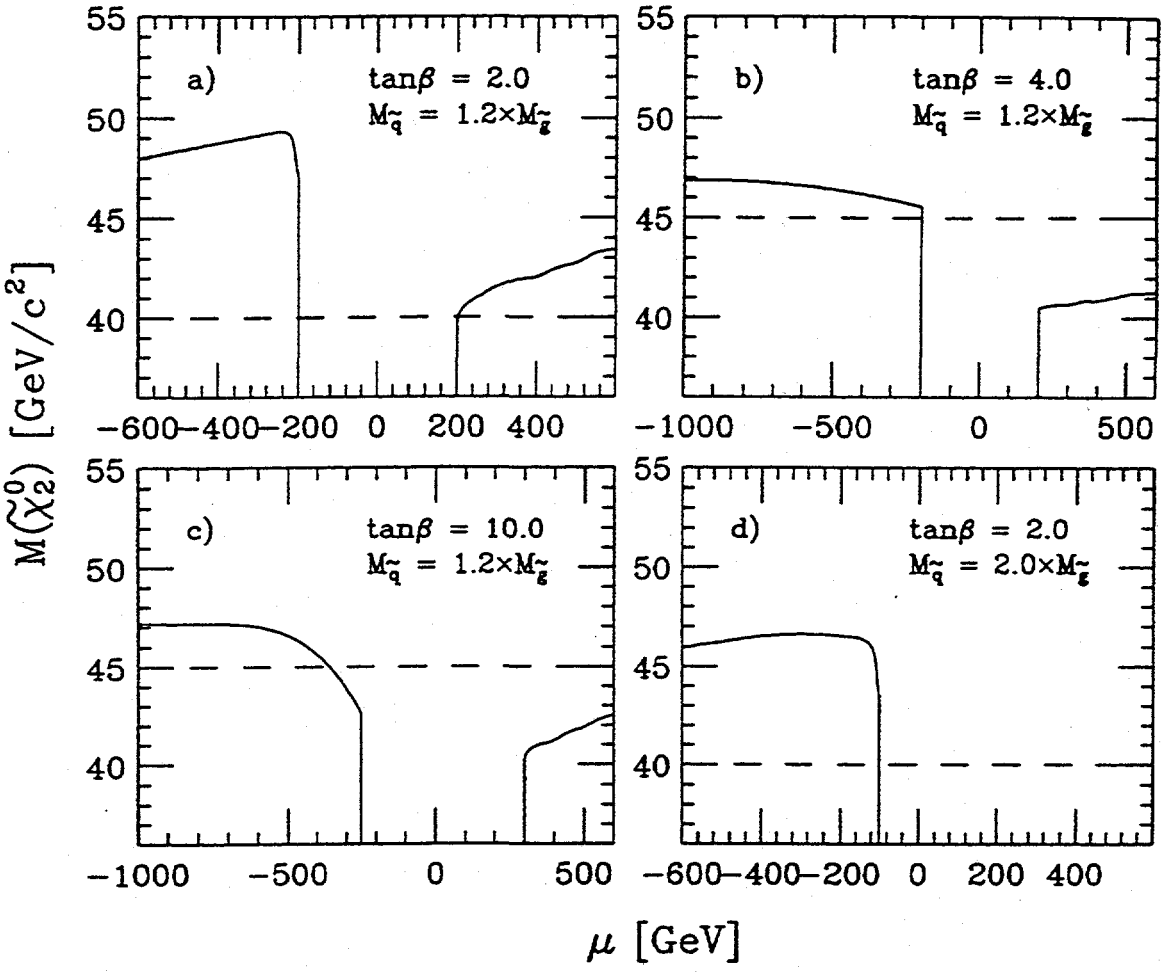

Figure 3: Neutralino mass lower limits obtained in the trilepton analysis (solid line). The SUSY parameters used for each plot were: a) tanβ=2.0, $M_{\tilde{q}}$=1.2; b) tanβ=4.0, $M_{\tilde{q}}$=1.2; c) tanβ=10.0, $M_{\tilde{q}}$=1.2; d) tanβ=2.0, $M_{\tilde{q}}$=2.0. The dashed line is the limit extracted from LEP measurements. Note that μ only extends down to -600 GeV for tanβ=2.0.

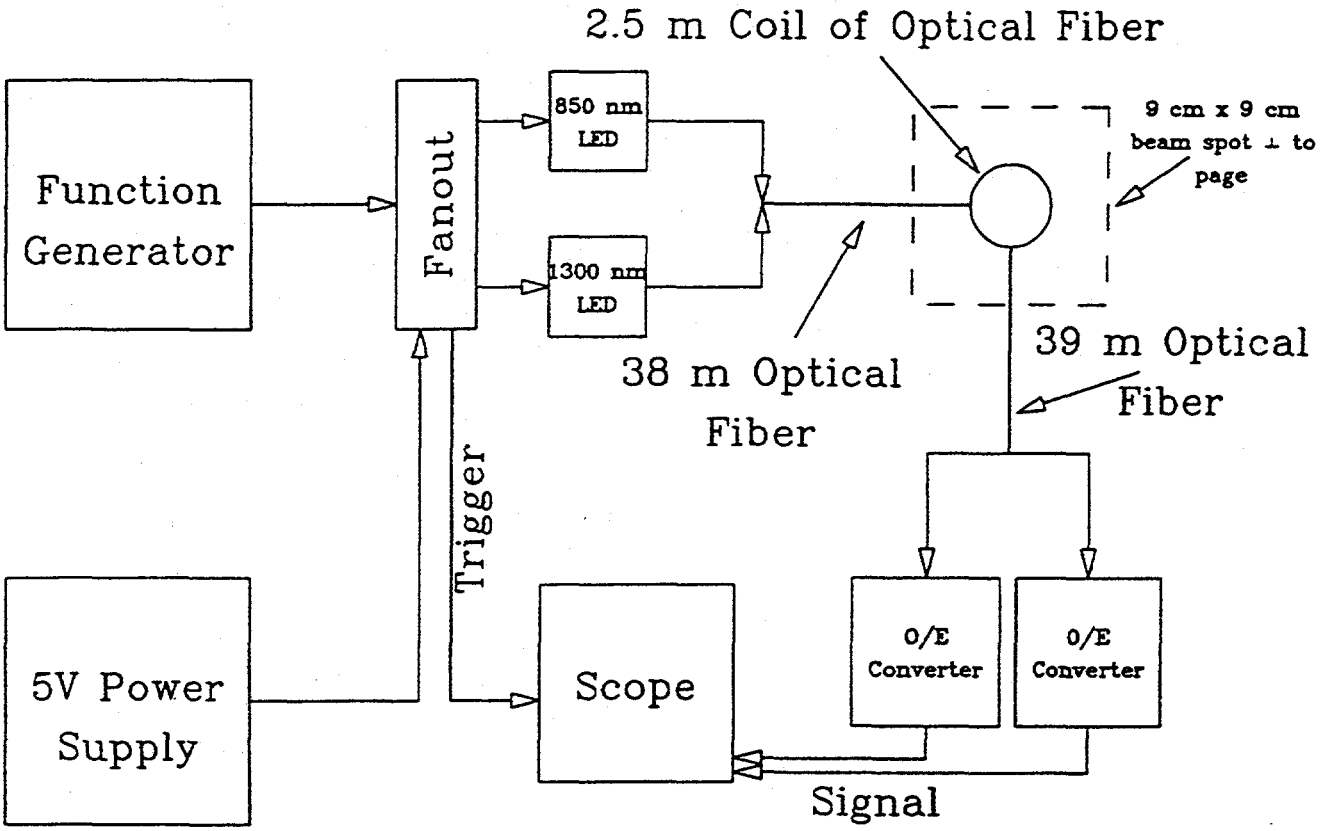

Figure 4: Experimental setup. The fiber was continuously pulsed during the entire run. V_{pp} was measured using the scope and recorded hourly.

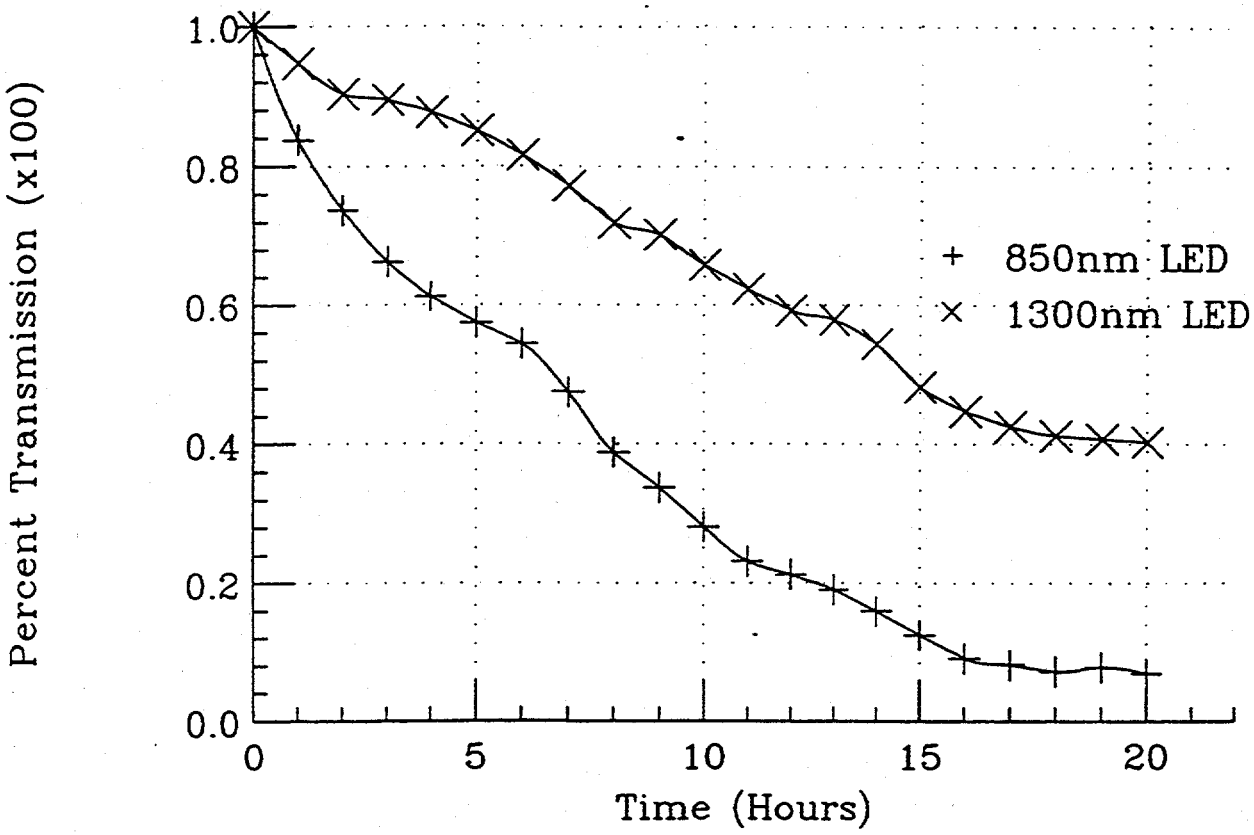

Figure 5: Plot of percent transmission versus time. Our dose measuring devices failed sometime during the run and exact dosage versus time is unknown. However, the total delivered dose is 200 kRad, more than twice the expected lifetime dose of the fiber. As the lasers we plan to use have a wavelength of 1550 nm, we expect to see even less radiation damage.

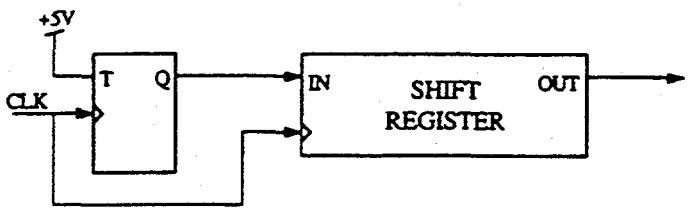

Figure 6: Block diagram of the circuit programmed inside the Actel parts.

II. The MACRO Experiment

The MACRO experiment staged at the Gran Sasso Laboratory in l'Aquila, Italy is one of the next generation underground, large surface area experiments designed to study magnetic monopoles, astrophysical neutrino sources and other cosmic ray phenomena. This detector has already begun to provide us with a view of particle physics phenomena well above the window of energy soon to be opened by projects like the LHC, and as such represents a very important aspect of future research in high energy physics[1]. The details of the detector layout are shown in a schematic view of the completed detector presented in Figure 1, and the details of the physics program and the capabilities of this detector have been presented in previous renewal requests to the DOE as well as in the original scientific proposal[2].

In the past year the MACRO experiment has at long last been fully instrumented and is now ready to begin the *push* toward the "Parker Limit"[3] in its search for super-heavy GUT magnetic monopoles. During the summer of 1995 the final touches were placed on the waveform digitizing system and the slow monopole trigger system and beginning in early fall, the full detector began taking "slow monopole" data along with the standard set of muon and stellar collapse triggers. This marks a significant milestone in the evolution of the MACRO experiment and begins the five year campaign to collect the monopole data originally proposed.

In the sections that follow, we will discuss the progress being made on physics analyses being carried out at Texas A&M as well as present our plans for the coming funding cycle.

A. Current MACRO Physics Results

One of the most exciting analyses that is currently being carried out by the collaboration is the search for upward going muons in our data sample. This class of events is particularly interesting since they must arise from neutrino interactions in the rock below. Hence, we may use this data sample as a probe for various sources of high energy neutrinos (e.g., neutrino oscillations, neutrino point sources,

WIMP annihilation and dark matter searches). Since the last time we reported on this work MACRO has been able to collect almost twice the amount of data contained in our first upward going muon work. This increase in statistics will enable us to probe further the physics issues which these events involve. In the sections which follow, we describe the status of the analysis effort on this event sample being carried out by A. Sanzgiri of our group.

Upgoing Muon Analysis of Recent Data

An upward-going muon analysis has been performed on the data collected during the running period: 16 March 1994 - 3 May 1995. This corresponds to 0.97 live-years of data collected with the lower supermodules as well as the "ATTICO". The dataset analysed consists of 1455 good runs of lengths greater than 1 hr. between runs 7244 and 9908. Approximately 5.1 million single muons passed all analysis cuts and 156 muons were identified as upgoing in the $1/\beta$ range $-1.2 \leq 1/\beta \leq -0.8$.

The analysis procedure employed was to match tracks in the streamer tubes with clusters of scintillator boxes that were "hit" (i.e boxes which triggered the ERP muon trigger). The velocity of the muon (and consequently its $1/\beta$) is determined from the pathlength of the muon and the relative time between ERP hits at the extremities of the muon's path through the detector. With the introduction of the "ATTICO", it is possible for a muon to pass through more than two planes of scintillator. The pathlength chosen was the projection of the streamer tube track to the center of scintillator planes containing the hit boxes that are farthest apart. The relative time between the box hits is determined from the raw TDC values reported by the ERP trigger. Muons passing through adjacent supermodules were also considered - here the relative time determination uses in addition TDC values obtained from the interERP electronics.

To reduce background due to multiple muons, stopping muons, showering events, coincident radioactivity etc. a variety of cuts were employed: we required that there be less than 10 scintillator box hits, up to 4 clusters and a single track in the event; the range of acceptable TDC values was set to be 1500 - 4000 and we insisted on an agreement between the projected track and the position determined from the ERP TDCs. Additionally, we imposed a minimum pathlength requirement of 2.5 meters to ensure that the time of flight is significantly longer than the intrinsic timing resolution of the scintillator system. Scintillator boxes,

supermodules or their combinations were excluded from the analysis on a run-by-run basis if they suffered from hardware or calibration problems.

In Figure 2, we show the resulting $1/\beta$ distribution after all analysis cuts have been applied. A clear peak of upgoing muons centered at $1/\beta = -1$ is evident. Assuming a Gaussian distribution of $1/\beta$ for upgoing muons, the range $-1.2 \leq 1/\beta \leq -0.8$, corresponds to 4 standard deviations, and was used to define our selection of upgoing muon candidates. A background estimate was performed using the events present in the range $-0.8 \leq 1/\beta \leq 0$. The detected number of upgoing muons after background subtraction is $146 \pm 12_{sys}$.

Comparison with Monte Carlo Calculations

Over 250,000 simulated upgoing events were generated using GMACRO (the detector simulation code) and a muon flux table produced by S. Mikheyev. The muon fluxes are based on the 'Bartol' atmospheric neutrino flux [4], use cross-sections for neutrino interactions calculated from the parton distributions of Morfin & Tung [5], the propagation of muons to the detector is done using the energy loss calculations of Lohmann *et al* [6] for standard rock, with a $\nu/\bar{\nu}$ ratio set at 1.25. The simulated events were subjected to the same analysis procedure as was used for the real data. The expected number of upgoing muons in one year is 186 for a fully efficient detector, with a systematic error of about 15% (mainly arising from the uncertainty in the atmospheric neutrino flux).

For brief intervals during this running period, some supermodules were turned off for phototube gain-setting. In addition, the interERP circuitry was not in operation or had hardware/calibration problems especially towards the beginning of this running period. To calculate the effective livetime of the apparatus, a subset of runs from run 9000 - 9278 when the detector was almost fully efficient were used as "reference" runs. Comparing the number of muons passing the analysis cuts in the reference sample with those in the entire dataset, the effective livetime of the apparatus was determined to be 0.87 years. This leads to an expectation of $156 \pm 23_{sys}$ upgoing muons from Monte Carlo calculations.

A comparison of the zenith angle distribution of upgoing muon events from the real data and the simulated sample is shown in Figure 3.

Upward Muons: Summary and Future Outlook

The measurements being reported on in the previous section are planned as the Ph.D. dissertation subject matter for Mr. Sanzgiri of our group. We anticipate that this work will be completed by the spring of 1996. Also as we mentioned earlier these new data on the flux of upward muons will allow us to probe a wealth of physics topics. With this enlarged data sample, we will be able to set new and stronger limits on astrophysical point sources of neutrinos; set improved constraints on neutralino dark matter and the possibility of neutralino decay; as well as attempting to study neutrino-oscillations in the atmospheric neutrino flux. Our group will continue working with the collaboration on this area of analysis over the course of the coming year.

B. Monopole Searches with MACRO

As mentioned earlier, one of the highest priorities in MACRO's physics program is to search for magnetic monopoles with a sensitivity below that of the astrophysically inferred "Parker Bound" and with the completion of the WFD system we are poised to initiate such a search with MACRO. As you know, this bound places an indirect limit on magnetic monopoles abundances based on the existence of intergalactic magnetic fields. Since magnetic monopoles passing through these regions of magnetic field would gradually reduce these field strengths, it is argued that the existence of such fields mean that monopoles are not abundant enough to remove the energy being stored in these magnetic fields by the cosmic dynamo mechanism giving rise to these fields. Using typical values of these field strengths, regeneration times and dimensions of these regions, Parker, Turner and Bogden[7] came up with an upper bound for monopole fluxes of 10^{-15}cm^{-2}sr^{-1} sec^{-1}. Recently this limit has been further refined to include more detailed aspects of the magnetic field generation yielding a modified bound of 1.6 x 10^{-16} cm^{-2}sr^{-1}sec^{-1}.[8]

The MACRO detector's size was chosen to be able to push the limit for monopole abundances to this level and below. For the full MACRO detector including "ATTICO" with an acceptance of 10,000 m^{2}sr, the "Parker Bound" corresponds to a sensitivity of about three monopoles per year passing through the detector.

MACRO uses primarily the ionization properties of these slow moving mono-

poles for detection. Here the moving magnetic charge produces a transverse electric field due to its motion, where the strength of this field is velocity dependent. At ultra relativistic velocities the monopole's electric field is larger than that of a relativistic charged particle by $(n^2g^2 \sim n^2 4700)$. Hence, making high velocity monopoles as easy to detect as fast moving heavily ionizing particles. At the other end of the velocity spectrum, as the monopole's velocity goes below 10^{-3}c, there is a rapid falloff in the specific ionization. At these low velocities we expect to see monopoles as lightly ionizing, slow moving particles.[9]

To trigger on monopoles throughout this entire velocity range is quite a challenge. In order to accomplish this we have reverted to a combination of triggers specifically tailored to each of three velocity ranges:

1) Fast monopoles, $\beta > .1$;
2) Intermediate velocity monopoles, $10^{-3} < \beta < .1$;
3) Slow monopoles, $10^{-5} < \beta < 10^{-3}$.

For each of these triggers we take advantage of the timing aspects as well as the expected pulse height of the monopole signal to optimize these triggers. For the slowest velocity range, the job is most complex so I will briefly describe it here. In this range we expect monopoles to take of order 1μsec or more to transverse a scintillation counter. As a monopole moves along its path through the scintillation liquid, it deposits small amounts of energy in the scintillator which yields small amounts of light spread over this time interval. The trigger used here has a "leaky integrator" to add up these faint signals over the traversal time through the scintillation counter. The time constants of the integrator are chosen to match the velocity range of interest.When there is enough energy deposited while a monopole candidate is traversing a counter to cause the leaky integrator signal to pass a predetermined threshold before it discharges, a monopole trigger is generated.

With the completion of the WFD system and the accompanying trigger hardware, we are now able to begin these monopole searches. As a result, the coming five year running period will be a very exciting and rewarding time for this program.

C. Plans for the Next Funding Cycle

The TAMU team composed of Dr. R.C. Webb, graduate student Ashutosh Sanzgiri and technician A. David will be responsible for the ongoing maintenance

of the wfd and scintillator high voltage systems as required. In addition to our work on the WFD system and continuing to maintain various general electronics systems, we will also be continuing our work on the off line analysis of the MACRO data. With the detector now fully operational, our future efforts will focus on the physics program of the upward going muons mentioned earlier and the search for magnetic monopoles to the "Parker Bound"[3].

References

1. Drell, S. *et al.*, *High Energy Physics Advisory Panel's Subpanel on Vision for the Future of High-Energy Physics*, **DOE/ER-0614P**, May 1994(unpublished).

2. The MACRO Collaboration, *Proposal for a Large Area Detector Dedicated to Monopole Search, Astrophysical and Cosmic Ray Physics at the Gran Sasso Laboratory*, November, 1984 (unpublished).

3. Parker, E.N., *Cosmological Magnetic Fields,* (Clarendon Press, Oxford) (1979) 15.

4. T. Gaisser, private communication.

5. Morfin, J.G. and Tung W.K., Z. Phys. **C52** (1991) 13.

6. Lohmann, W., *et al.*, CERN-EP/85-03, Mar, 1985.

7. Turner, M.S., Parker, E.N., Bogdan, J.T., Phys. Rev., **D26** (1987) 1296.

8. Adams, F.C., *et al.*, University of Michigan Preprint **UM- TH-93-04** Submitted *Phys. Rev. Lett.*

9. Ahlen, S.P. and Tarlé, G., *et al.*, Phys. Rev., **D27** (1983) 688.

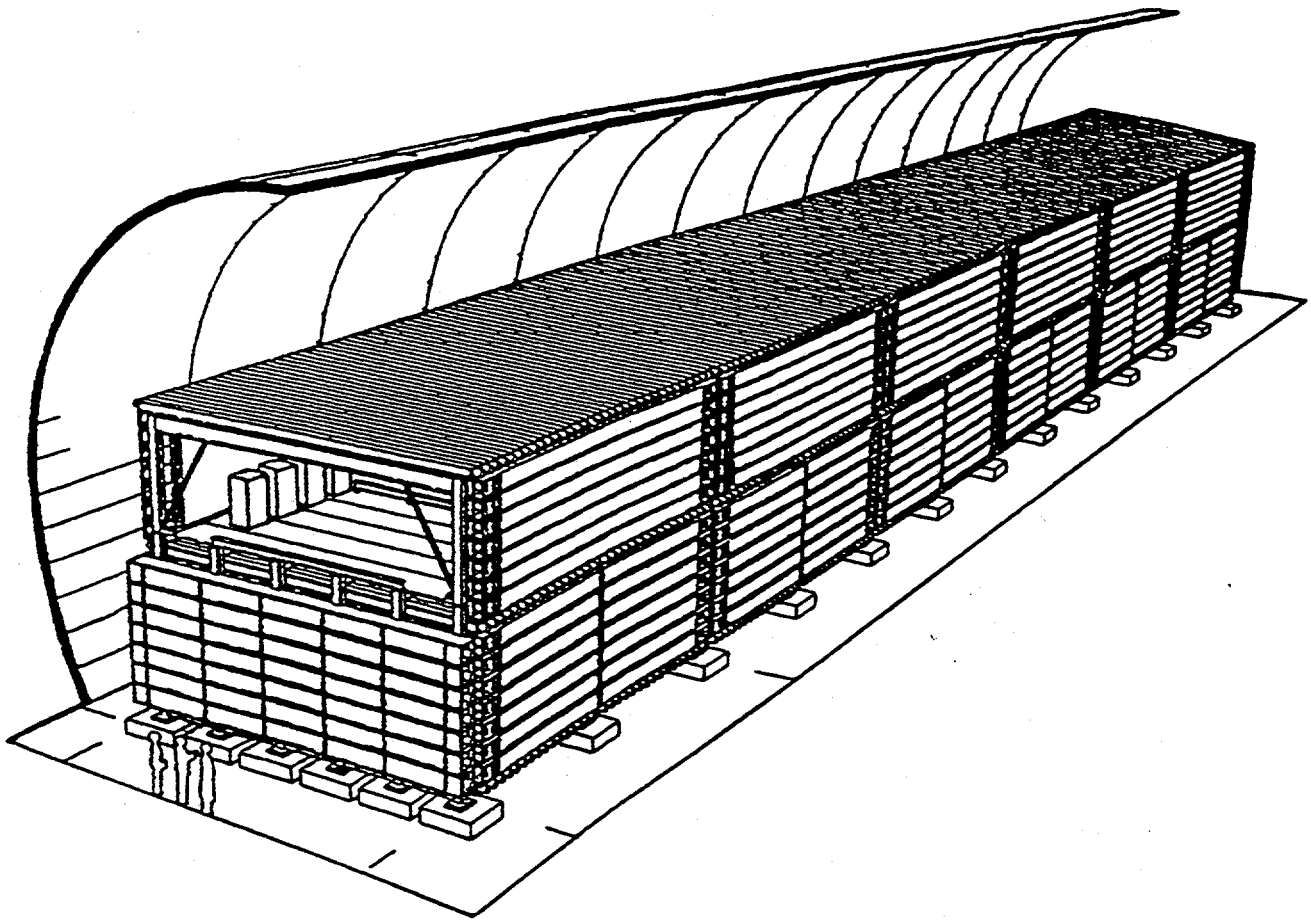

Figure 1. Layout of the MACRO detector showing the six supermodules with the Attico.

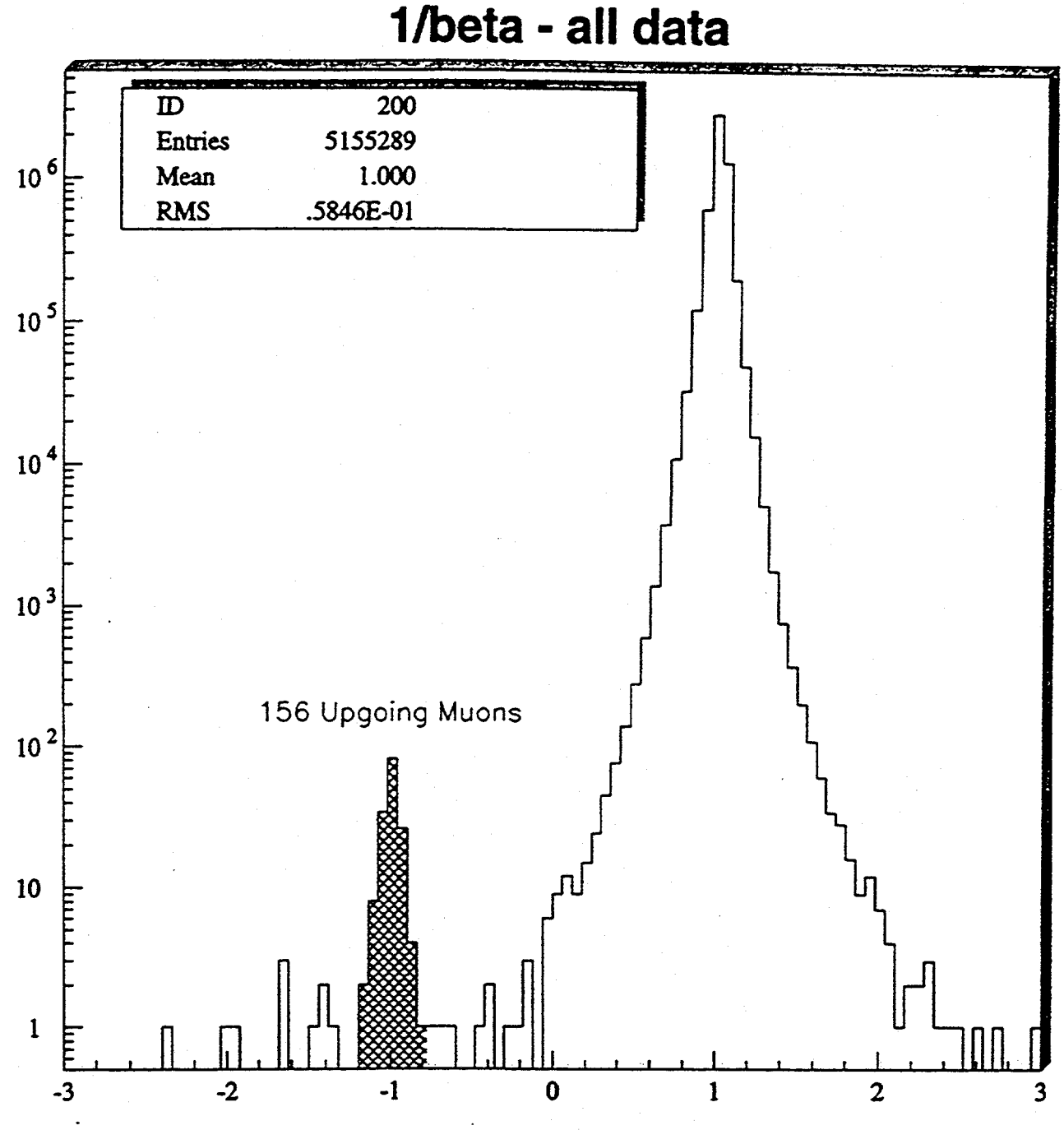

Figure 2. $1/\beta$ distribution of muons in the analysed data. The number of upgoing muons in the $1/\beta$ range $-1.2 \leq 1/\beta \leq -0.8$. is 156.

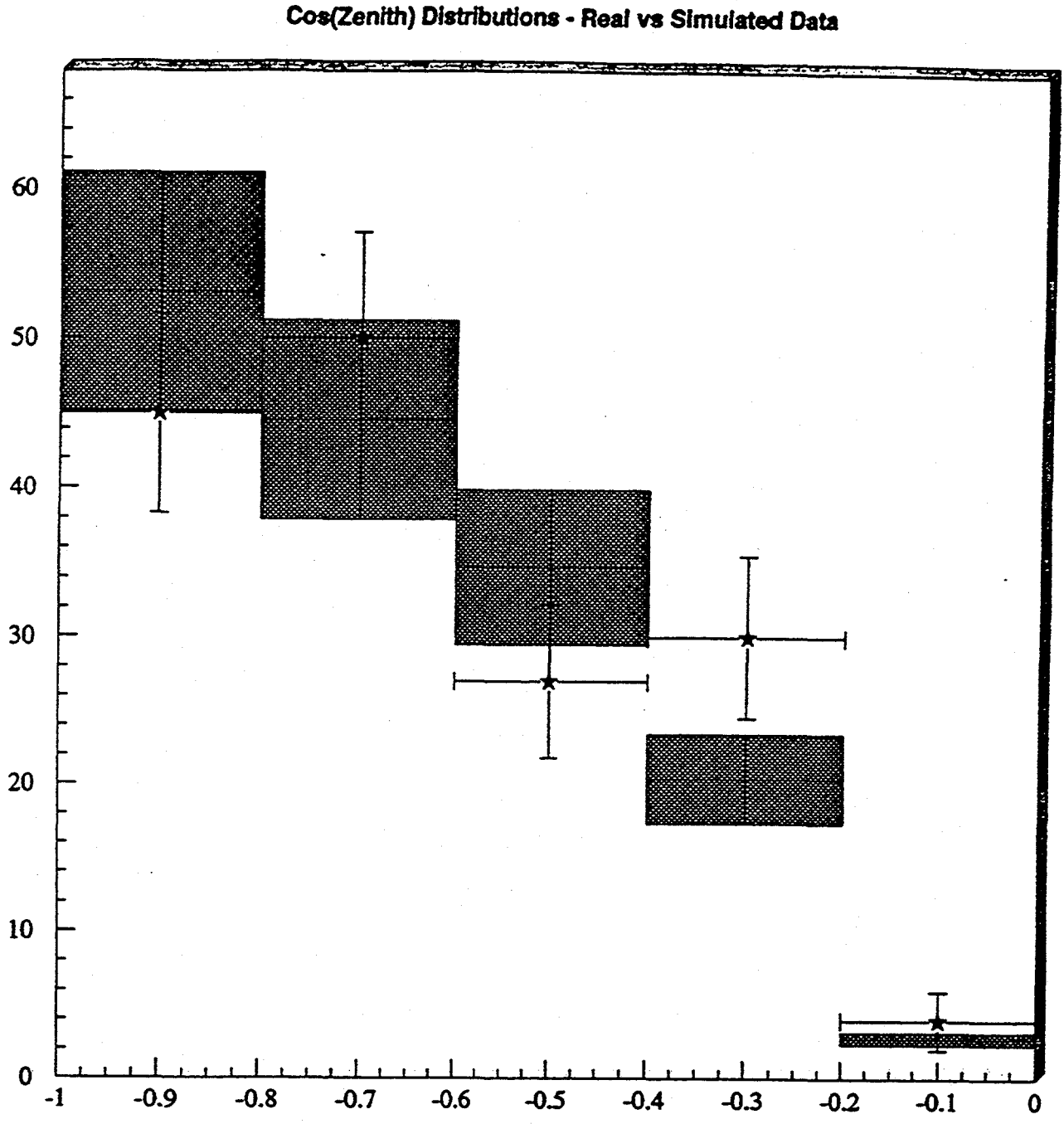

Figure 3. Zenith angle distributions for upgoing muons in the real data compared with MC expectations. The upgoing events in the real data (without background subtraction) are shown as stars along with their statistical errors. The expected events are shown as rectangular boxes reflecting the 15% systematic uncertainty in the Monte Carlo.

III. Long Baseline Neutrino Program(MINOS)

As part of the evolution of our MACRO program, we have been involved in the development of an *Expression of Interest*[1] and a Fermilab proposal[2] for a large fine-grained magnetic sampling detector to be used for studying events induced by accelerator or atmospheric neutrinos for the purpose of searching for neutrino oscillations. The MINOS Collaboration has evolved substantially over the past calendar year and was able to submit within a rather accelerated time frame a proposal for a long-baseline experiment using a beam from Fermilab and a new detector in the Soudan iron mine in northern Minnesota. This detector (see Figure 1) would allow the study of a number of possible signatures for neutrino oscillations based on disappearance of muon neutrinos, ratio of neutral current to charged current events and appearance of tau or electron neutrinos by additional electromagnetic showers or apparent 'neutral current' events giving hadronic showers in the detector. Most importantly, the detector being contemplated would provide an unambiguous signature of tau appearance using the muon decay channel of the tau, particularly if a narrow-band beam is employed.

The proposed detector would also represent a major stand-alone underground detector facility for non-accelerator physics which would naturally dovetail with our current MACRO program. With such a detector atmospheric neutrinos could also be collected during the same period as beam measurements are made and allow an extension of sensitivity to smaller Δm^2 using the ratio of neutral current to charged current events; a new physics signature for atmospheric neutrinos. In addition to the neutrino physics, a detector with these capabilities will also be able to extend current physics measurements on other non-accelerator topics including: measurement of momenta for both downgoing and upgoing muons up to hundreds of GeV momentum; precise timing measurements over a large detector for differences in arrival time of muons within a bundle; rough measurement of very high muon energies based on bremsstrahlung and pair production; search for very high energy muons at large zenith angles; and other topics. In this section we will briefly outline the physics objectives of this program and how we plan to participate in this program.

A. Physics Objectives of the Long Baseline Program

Observations by the Kamiokande and IMB collaborations on contained neutrino-induced events in their detectors suggest that perhaps as much as 40% of atmospheric muon neutrinos in the energy range 0.2-1.5 GeV are missing. [3,4]. The possibility of muon neutrino to tau or electron neutrino oscillations could explain the deficit. The atmospheric neutrino data suggest particular regions of mixing parameter space to explore. Figure 2 shows the regions of oscillation space which are allowed at the 90% confidence level from the Kamiokande measurements. Here, we assume that a minimum requirement for a significant new experiment should be an ability to clearly observe neutrino oscillation signatures for the regions suggested by the atmospheric neutrino anomaly. However, we do not think that we should be limited to that region of parameter space. Rather, we wish to achieve sensitivity to the largest region of parameter space possible, given reasonable constraints on current accelerator beams and cost of the detector. We set a particular goal of reaching $\sin^2 2\theta = .01$ for large Δm^2 ('fully mixed'). However, because of the hint coming from the atmospheric neutrinos, we believe that marginal gains in sensitivity in parameter space should not come at the cost of excellent understanding of systematic errors in the region of the atmospheric anomaly.

The issue of systematic error in a long-baseline experiment is of crucial importance. Detectors which are far from an accelerator will necessarily be very large. The acceptance for some particular physics signature can be well understood by study of some small section of the full detector in an accelerator beam-test. However, it is unlikely that the acceptance for the full detector will be as well demonstrated as might normally be the case for an accelerator experiment. In addition, the extrapolation of neutrino beams to very large distances is not a 'well known and measured' technique. Detectors which are very distant from the accelerator typically will have significantly different beam spectra than those at near or intermediate distances. Small divergence effects which are normally of no consequence for near accelerator experiments will become important for the long-baseline experiment. This will impose an irreducible systematic error on an experiment which relies solely on ratios of events in near and far detectors. The uncertainty in the beam at the far detector will also give systematic uncertainty to any physics signature based on some absolute calculation of an expected number of events. Finally, any measurements made with the atmospheric neutrinos

will always have a number of systematic errors arising from uncertainty in the direction, flux and energy of the incoming neutrinos.

In order to make the most convincing experiment possible, we take three basic approaches to measurement of neutrino oscillation parameters. First, we wish to make the measurement using a number of different physics signatures. Since the measurements all make use of the same beam, they are not completely free of correlated systematic error. However, the systematic errors for the different measurements will largely be uncorrelated. We should be able to require consistency between the measurements. Second, whenever possible, we use ratios in order to limit the systematic errors involved in absolute normalizations. Finally, we wish to demonstrate clear appearance signatures for the neutrino flavor which the muon neutrinos have oscillated to. For electron neutrinos, this means identification of the electron in charged-current interactions. For tau-neutrinos, we know of no means of either explicitly reconstructing the tau mass or of observing a secondary vertex resulting from the tau decay in a very large detector. Hence, we resort to statistical means to identify tau appearance based on the different possible tau decay modes.

B. Current and Planned Involvement

The MINOS Experiment has been evolving at a very rapid pace over the past twelve months. In early February, the collaboration completed and submitted its proposal to the Fermilab PAC for review. This plan received strong support from the lab and received STAGE 1 approval from the PAC at this meeting. Following soon thereafter the DOE asked for a HEPAP subpanel to be convened to advise it on "Accelerator-Based Neutrino Oscillation Experiments", since these programs had not been included in its earlier long range planning for HEP. The collaboration prepared extemsively for this review, which was carried out during the past summer, since it was effectively a *shoot-out* between our proposal and a competing proposal from BNL. In the final report from the subpanel published in late September, the MINOS program was given high marks for its program and the recommendation to DOE was to move forward with this program. Once this final hurdle was cleared, the MINOS team has been able to get back to working on the R&D necessary to carryout this project which had been put on hold until this review was completed.

Over the past year the TAMU team has focussed its attentions on Monte Carlo simulations of the detector and studies of several of the important physics

signatures of the detector. This work was being carried out by Dr. H.-J. Trost, however as of December 1, 1995, funding for Dr. Trost's position was exhausted and he has since left our program. During the time that Dr. Trost was able to devote to this project during the past year he was able to make several important contributions to the simulations effort.

In addition to this simulation work, we have also become involved with the R&D effort on the development of a scintillator-based detector design for the *far* detector. This work follows closely some of the work that our group had undertaken as part of its SSC R&D program[5] over the past several years. To that end we have set up a test stand to test prototype scintillation detectors for MINOS here at TAMU. These devices are essentially liquid containers of either aluminum or plastic, with a cross section of 2.0 X 2.0 cm and 8.0 m in length, which we fill with a suitable liquid scintillator. The scintillation light is then readout using a wavelength shifting fiber stretched down the axis of this 8 meter long tube. The MINOS *far* detector will have nearly 500,000 such tubes, and we are studying the response properties of these prototypes to cosmic rays and ultimately to hadronic showers. Our test stand is complete with a cosmic ray trigger telescope and a PC-based CAMAC data acquisition system which should allow us to carryout detailed studies of the response function of various prototype detector configurations. With the departure of Dr. Trost from this effort, our plans for the coming year will have us focussing on the scintillator R&D effort almost exclusively.

References

1. B. Barish *et al.*, *Expression of Interest for a Long Baseline Neutrino Oscillation Experiment using a Main Injector Beam and a Large Magnetic Sampling Calorimeter* , May 16, 1994, Submitted to Fermilab, NuMI-L-9(unpublished).
2. D. Ayres *et al.*, *MINOS Proposal*, February 9, 1995, submitted to the Fermilab PAC, NuMI-l-63(unpublished).
3. K. S. Hirata *et al.*, Phys. Let. **B280** (1992) 146.
4. D. Casper *et al.*, PRL **66(20)** (1991) 2561.
5. M. Gui *et al.*, *Liquid Scintillating Fiber Calorimeter Prototype*, submitted to the IEEE Trans. Nucl. Sci., October 1994.

MINOS Far Detector
in the Soudan mine

600 layers of 4 cm Fe + 2 cm gap
10 kT total mass
Toroidal magnetic field <B> = 1.5 T

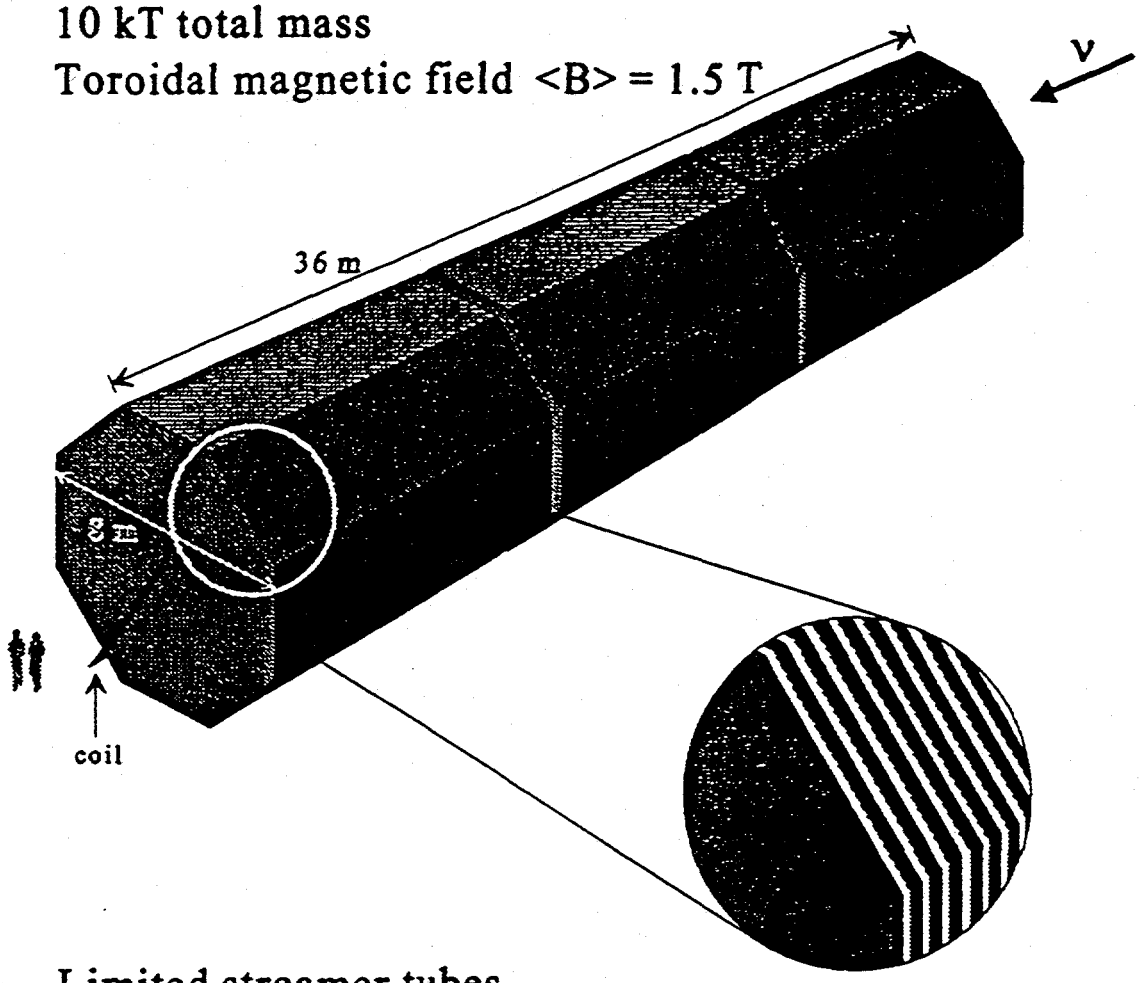

Limited streamer tubes
32,000 m² active area
wire and cathode strip readout, 480,000 channels

Figure 1. Schematic drawing of the MINOS far detector.

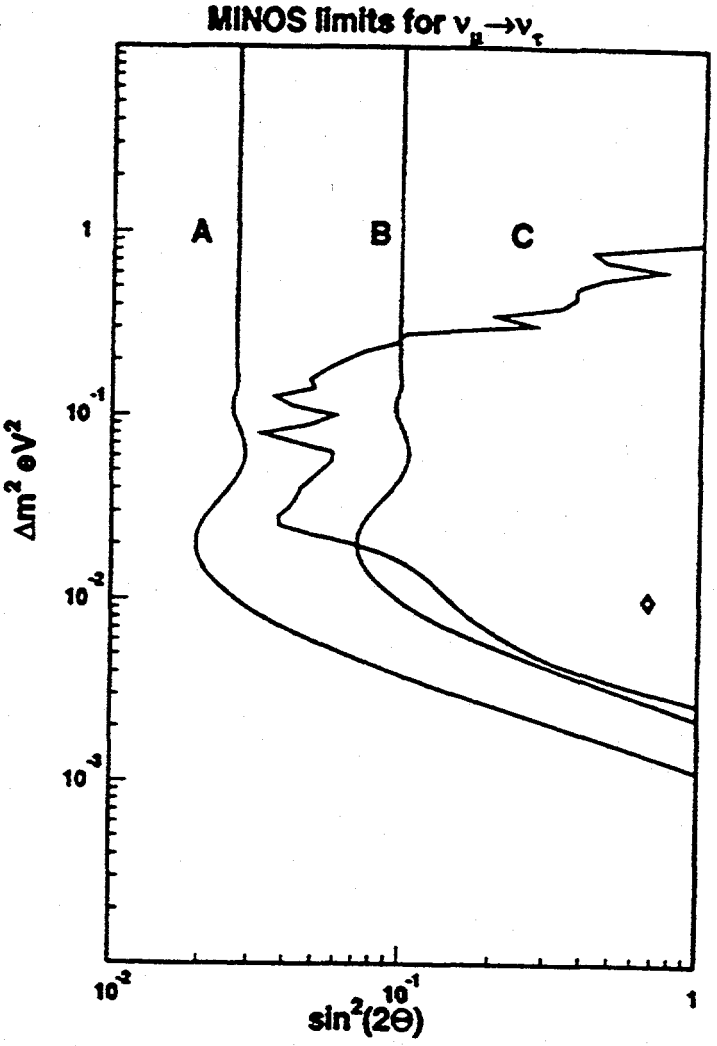

Figure 2. Regions of neutrino oscillation space allowed by the Kamiokande measurement with the *reach* of the MINOS Experiment based on 2 years of running overlayed.

IV. Theoretical Physics Program

A. Research by D. V. Nanopoulos

1 Introduction

During the past year I have been involved in several projects, ranging from hard-core phenomenology to studies of non-perturbative string effects, including stringy black holes. The underlying theme of my research has always been the construction of a realistic string model according to

string dynamics at the Planck scale, and its possible testable predictions at low energies. Clearly, such a formidable task cannot be achieved easily and needs a lot of information from almost any branch of string theory and phenomenology. As such, I have taken the following lines of research:

1. String theory
2. Model building
3. SUSY phenomenology
4. Astroparticle Physics
5. Brain function and quantum mechanics

1.1 String Theory

1.1.1 Non-perturbative String Theory

During the last few years we have developed a program for studying non-perturbative string dynamics, including quantum fluctuations of the space-time metric, that has produced some interesting results, see *e.g.*, [1]. In this framework, we have given some explicit examples [2], at least in two space-time dimensions, that we may need to go a bit further than S-matrix formalism of conventional point-like quantum field theory. An amazing consequence, as we have stressed for some time [3] is the possibility of CPT violation. Recently we have worked out [4] in considerable detail the predictions of our stringy CPT-violation for the $K^0 - \bar{K}^0$ system, presently under experimental study at CP-LEAR at CERN and at Fermilab. Furthermore, we joined forces with the CP-LEAR collaboration and provided [5,6] the best available limits on possible violations of Quantum Mechanics and CPT violation, at the level of $\mathcal{O}(10^{-19})$, which is exactly where we expect quantum gravitational effects $\mathcal{O}(G_N m_K^2 \sim 10^{-19})$ to kick in. Improvements of the present limits are expected in the near future from experiments at CERN and Fermilab, and in a few years

from the DAΦNE experiment at Frascati. Clearly, observation of CPT violation will signal the official opening of a new era in the microworld.

1.1.2 Perturbative String Theory

Efforts to build a viable string unified theory continue untames. We have provided an explicit formula for the number of generations in free-fermionic string models, that accepts a geometrical interpretation and connects to the corresponding formula (in terms of the Euler number) of Calabi-Yau manifolds [7]. We have worked out [8] in detail the conditions under which we can derive No-Scale Supergravity theory (see *e.g.*, [9]) in string theory, as it should be expected. Furthermore, we have proposed a new generic mechanism [10] involving the endemic (in string theory) "anomalous" U(1), realizing the vanishing of $\mathrm{Str}\mathcal{M}^2$. It should be emphasized that the above recent developments have provided us with further ammunition for the construction of realistic string models.

1.2 Model Building

The availability of a better understanding of perturbative string dynamics has prompted us to take a fresh look at one of the most realistic string models, namely flipped SU(5) (see *e.g.*, [11,12]). Indeed, we found [9,10,11] that there is a version of flipped SU(5), that in Ref. [13], that satisfies all the conditions discussed in Section 1.1.2 above, and thus makes a prime candidate for a viable Grand Unified String Theory (GUST). Furthermore, we proposed a new scenario [14] where all scales, including the LEP unification scale ($\sim 10^{16}\,\mathrm{GeV}$) are obtained dynamically and naturally. In a way, flipped SU(5) is the only model we are aware of that can accommodate and shed light on the existence of the LEP unification scale ($\sim 10^{16}\,\mathrm{GeV}$) and the string scale ($M_{\mathrm{str}} \sim 5 \times 10^{17}\,\mathrm{GeV}$).

On a different front, we have presented a complete SU(5) supergravity model, the so-called Missing Doublet Model (MDM) [15], which is based on a model first proposed more than ten years ago [16]. Sometimes the contrast between different models (in our case flipped SU(5) versus MDM) is very helpful to appreciate some virtues that by now are taken for granted!

1.3 SUSY Phenomenology

A better understanding of string model building at the Planck scale implies, in principle, a better understanding of the experimental consequences of such string models at low energies. Our strategy here has been multifold. To start with, we have implemented [17] the constraints from the "observed" $b \to s\gamma$ rate on generic supergravity models, as well as studied their contributions to $R_b = \Gamma(Z \to \bar{b}b)/\Gamma(Z \to \mathrm{all})$ [18], taking into account [19] even the latest limits on SUSY particles from LEP 1.5.

We found that while $b \to s\gamma$ can be easily accommodated in SUGRA models, the experimental value of R_b cannot be reached in SUGRA models [19]. In the next step we implemented [20,21,22] all the above found constraints on a particular class of string no-scale supergravity models, close to our theoretical interest, and got a rather constrained SUSY spectrum. At least for the class of models we studied, a rather "light" SUSY spectrum emerged, that can be presently tested at Fermilab through dilepton/trilepton signals [23] or at LEP 1.5-2 through "light" ($< 90\,\mathrm{GeV}$) charginos, selectrons ($< 50\,\mathrm{GeV}$), and Higgs particles ($< 90\,\mathrm{GeV}$).

For the first time, and under plausible assumptions, we may be able to test experimentally stringy models, and may be able to refute or vindicate them. In addition, we noticed [23] recently that the LEP observed unification of strong and electroweak interactions fits much more nicely in the flipped SU(5) model, by avoiding the conflict between $\alpha_s(M_Z)$ and $\sin^2\theta_W(M_Z)$ and even opening the way for reconciliation between

low-energy ($Q \ll 100\,\mathrm{GeV}$) and LEP ($Q \sim 100\,\mathrm{GeV}$) determinations of $\alpha_s(M_Z)$, with the possibility of observable proton decay ($p \to e^+\pi^0$) at SuperKamiokande [23]. Evidently the next few years will be crucial for the viability or not of stringy derived effective supergravity models.

1.4 Astroparticle Physics

Supersymmetric models predict, generically, the existence of a stable neutral particle as the lightest one in the Superworld, the Lightest Supersymmetric Particle (LSP) [24]. LSPs may serve as prime candidates for Dark Matter. In Ref. [25] we calculated the prospects for detection of flipped SU(5) LSPs in the lab, and found that in this case flipped SU(5) dark matter is well hidden and rather difficult to observe. Furthermore, following present trends in observational cosmology (*e.g.*, recent observations by the Hubble Space Telescope (HST) yielding a rather large value for the Hubble parameter) we have proposed a new cosmological model [26] with a time-varying

cosmological constant, based on non-critical string theory [1]. While this model may resolve the possible potential problem of the age of the Universe, it also helps in "closing" the Universe [27], a prerequisite for inflation. In fact, we have recently proposed [28] a new dynamical model for inflation, based on non-critical string theory [1], where there is no need for "rolling" inflatons and extraneou fine tuning to achieve desirable results. The needed entropy is provided by the "friction" between observable degrees of freedom and stringy global states, that act as an environment. Finally, we have revisited [29] and reconfirmed our previous calculations [30] concerning the thermal regeneration rate for light gravitinos in the early universe, despite recent claims to the contrary.

1.5 Brain Function and Quantum Mechanics

On a project of much more interdisciplinary nature, I have put some effort to understand some functions of the brain based on subneural structures called Microtubules [31]. Indeed, we have found [32] that microtubule networks may be described by 2-D non-critical string dynamics, including the possibility of spontaneous decoherence that may be of fundamental importance in our conscious view of the world. In addition, we have proposed a new mechanism [33] for memory coding and recall, utilizing the infinite stringy symmetries available, thus avoiding the problem of limited memory capacity, endemic in models based in local field theories. Clearly, this field is in an embrionic stage and much more work is needed before even we can see the perigramm of an emerging theory of brain function.

2 Future Research

I plan to move on several fronts along the lines discussed above. We are going through a critical time for (critical) string theory. Finally it has hit home that critical string theory is only a small part of string theory, as we have argued for several years (see *e.g.*, [1]). Non-perturbative string effects are starting to be understood and 2-D stringy black holes seem to play a rather fundamental role. I plan to move on with our non-critical string theory approach and shed light (from our point of view) on recent developments concerning non-perturbative string theory that hold a lot of potential. On the stringy model building approach I plan to use more dynamical stringy properties in constructing an even more realistic flipped SU(5) model and work out all its phenomenological consequences at low energies. SUSY phenomenology, with forthcoming new results from LEP 1.5/Fermilab/LEP 2, promises to be a very "hot" subject and some work will be needed to implement the new limits/discoveries on the available realistic SUSY models. On the cosmological front, improvements on the error of the Hubble parameter, as measured by the HST, are eagerly awaited. Large values of H_0 will turn the tables on the Standard Big Bang Cosmology (too young a Universe!), and thus suggesting the need for amelioration of the Standard Big Bang Model, as the one suggested in [26]. I plan to work further in the consequences of such model with a time-varying cosmological constant, including possible ways to detect such a cosmological constant. Finally, on the brain front I plan to continue my program by making contact with the neural network approach, which from my angle emerges as an effective theory of the more fundamental microtubule networks. Also, I am already in contact with biophysicists/biologists, discussing ways that such ideas could be put under experimental scrutiny.

The next few years promise to be very exciting in all possible fronts: theory, phenomenology, cosmology, as more experimental data pour in, and as major advances

(after years of stagnation) are occuring in string theory.

References

[1] For a review see, D. V. Nanopoulos, "As time goes by ...", Rivista del Nuovo Cimento Vol. 17 issue no. 10 (1994).

[2] J. Ellis, N. Mavromatos, and D. V. Nanopoulos, Mod. Phys. Lett. A **10** (1995) 425.

[3] J. Ellis, N. Mavromatos, and D. V. Nanopoulos, Phys. Lett. B **293** (1992) 142 and CERN-TH.6755/92.

[4] J. Ellis, J. L. Lopez, N. Mavromatos, and D. V. Nanopoulos, Texas A & M University preprint CTP-TAMU-16/95.

[5] *Experimental tests of CPT symmetry and quantum mechanics at CPLEAR*, N. Mavromatos, *et. al.*, to appear in proceedings of the 2nd Dafne Workshop (DAΦNE 95), Frascati, April 1995.

[6] *Tests of CPT symmetry and quantum mechanics with experimental data from CPLEAR*, The CPLEAR Collaboration and J. Ellis, J. Lopez, N. Mavromatos, and D. V. Nanopoulos (to appear in Phys. Lett. B).

[7] I. Giannakis, D. V. Nanopoulos, and K. Yuan, Phys. Rev. D **52** (1995) 1026.

[8] J. L. Lopez and D. V. Nanopoulos, Texas A & M University preprint CTP-TAMU-60/94.

[9] A. Lahanas and D. V. Nanopoulos, Phys. Rep. **145** (1987) 1.

[10] J. L. Lopez and D. V. Nanopoulos, Texas A & M University preprint CTP-TAMU-37/95 (to appear in Phys. Lett. B).

[11] J. L. Lopez and D. V. Nanopoulos, Texas A & M University preprint CTP-TAMU-41/95.

[12] J. Lykken, `hep-ph/9511456`.

[13] J. L. Lopez, D. V. Nanopoulos, and K. Yuan, Nucl. Phys. B **399** (1993) 654.

[14] J. L. Lopez and D. V. Nanopoulos, Texas A & M University preprint CTP-TAMU-45/95.

[15] J. L. Lopez and D. V. Nanopoulos, Texas A & M University preprint CTP-TAMU-29/95 (to appear in Phys. Rev. D).

[16] A. Masiero, D. V. Nanopoulos, K. Tamvakis, and T. Yanagida, Phys. Lett. B **115** (1982) 380.

[17] J. L. Lopez, D. V. Nanopoulos, X. Wang, and A. Zichichi, Phys. Rev. D **51** (1995) 147.

[18] X. Wang, J. L. Lopez, and D. V. Nanopoulos, Phys. Rev. D **52** (1995) 4116.

[19] J. Ellis, J. L. Lopez, and D. V. Nanopoulos, Texas A & M University preprint CTP-TAMU-46/95.

[20] J. L. Lopez, D. V. Nanopoulos, and A. Zichichi, Int. J. Mod. Phys. A **10** (1995) 4241.

[21] S. Kelley, J. L. Lopez, D. V. Nanopoulos, and A. Zichichi, Mod. Phys. Lett. A **10** (1995) 1787.

[22] J. L. Lopez, D. V. Nanopoulos, and A. Zichichi, Phys. Rev. D **52** (1995) 4178.

[23] J. Ellis, J. L. Lopez, and D. V. Nanopoulos, Texas A & M University preprint CTP-TAMU-39/95.

[24] J. Ellis, J.S. Hagelin, D.V. Nanopoulos, K.A. Olive and M. Srednicki, Nucl. Phys. B **238** (1984) 453.

[25] X. Wang, J. L. Lopez, and D. V. Nanopoulos, Phys. Lett. B **348** (1995) 105.

[26] J. L. Lopez and D. V. Nanopoulos, Texas A & M University preprint CTP-TAMU-69/94 (to appear in Mod. Phys. Lett. A).

[27] J. L. Lopez and D. V. Nanopoulos, Mod. Phys. Lett. A **9** (1994) 2755

[28] J. Ellis, N. Mavromatos, and D. V. Nanopoulos, Texas A & M University preprint CTP-TAMU-12/95.

[29] J. Ellis, D. V. Nanopoulos, K. Olive, and S. Rey, Texas A & M University preprint CTP-TAMU-21/95.

[30] J. Ellis, J. Kim, and D. V. Nanopoulos, Phys. Lett. B **145** (1984) 181; J. Ellis, D. V. Nanopoulos, and S. Sarkar, Nucl. Phys. B **259** (1985) 175.

[31] D. V. Nanopoulos, Texas A & M University preprint CTP-TAMU-22/95.

[32] N. Mavromatos and D. V. Nanopoulos, Texas A & M University preprint CTP-TAMU-24/95.

[33] N. Mavromatos and D. V. Nanopoulos, Texas A & M University preprint CTP-TAMU-38/95.

B. Research summary 1995; C.N. Pope

My research in the calendar year 1995 has involved a number of topics. Some of these represent a continuation of an on-going research project involving a detailed study of various aspects of higher-spin extensions of conformal symmetry (W algebras), and their application to the construction of string theories with enlarged worldsheet symmetries. A related project involved an investigation of the BRST approach to the quantisation of the $N = 2$ worldsheet supersymmetric string, and its spectrum of physical states in two different descriptions of the 4-dimensional spacetime. More recently, my research has turned towards the investigation of the role of higher-dimensional extended objects (p-branes) in the perturbative and non-perturbative spectrum of string theory, with a view to gaining some insights into the duality symmetries relating strong and weak coupling in string theory.

1 W symmetries and W strings

Some time ago, the anomaly-free quantisation of a two-dimensional theory with local W_3 symmetry was carried out [1]. This paved the way to the construction of W_3 string theory, and its generalisations. The W_3 algebra, like all the finitely-generated W algebras, is non-linear, and so the quantisation of W_3 gravity and W_3 strings presents some new challenges that do not arise in the case of the Virasoro algebra and its supersymmetric extensions, notably in the way in which gauge fixing is implemented, and in the construction of the BRST operator. In previous work, we found a construction that provides a complete description of the physical spectrum of the W_3 string [2], and some generalisations to certain higher-spin W algebras. We also found a way to build BRST-invariant scattering amplitudes for the W string theories [3]. These results revealed deep connections between W-string theories and unitary minimal models.

In the last year, my work on W strings and W algebras was principally concerned with an understanding of the way in which less symmetric string theories can be embedded as special vacua of string theories with larger conformal symmetries. The idea was first proposed by Berkovits and Vafa, in the case of supersymmetric extensions of the Virasoro algebra [4]. They showed that the bosonic string could be viewed as a special vacuum of the $N = 1$ superstring, which could in turn be viewed as a special vacuum of the $N = 2$ superstring. They also suggested that some analogous hierarchy of embeddings might be possible for W strings. Recently, we succeeded in showing that the bosonic string could indeed be embedded as a special vacuum of the W_3 string [5], and the indications are that this is but the first of an infinite sequence of embeddings into higher W_N strings. An intriguing observation is that although the finite-N W_N algebras are non-linear, the $N \to \infty$ limit can be taken so as to yield the linear W_∞ algebra [6], which might lead to interesting

results as the limit is approached.

Another outcome of my recent work in the embeddings of string theories was an application of results in [7] on the linearisation of finite-N W algebras to construct simplified W algebras at certain special values of the central charge. We studied various examples, including some remarkably simple forms of the WG_2 algebra, which is generated by currents of spins 2 and 6, and is related to the exceptional group G_2 [8].

2 BRST Quantisation of $N = 2$ strings

The $N = 2$ worldsheet-supersymmetric string has always been somewhat of an enigma. For years, its critical dimension was not properly interpreted, and it was only relatively recently that it was appreciated that it describes a four-dimensional spacetime [9]. The drawback to this attractive-sounding property is that the $N = 2$ symmetry forces a grouping of the spacetime coordinates into pairs, leading to a $(2,2)$ spacetime signature. The $N = 2$ supersymmetry also requires that the spacetime be endowed with an additional invariant structure, which breaks the $SO(2,2)$ Lorentz group to a smaller subgroup. In the work of Ooguri and Vafa [9], the choice of a complex structure was made, breaking the Lorentz group down to $SU(1,1) \times SU(1,1)$. The physical spectrum of the theory turns out to comprise just a single bosonic degree of freedom. However, this is not a scalar field, but instead is the potential for a Ricci-flat Kähler metric on the four-dimensional spacetime. In fact, the theory in this formulation describes self-dual gravity [9]. In collaboration with H. Lu, I investigated the physical spectrum if an alternative additional structure on the $(2,2)$ spacetime is chosen, namely a real structure, which is invariant under $SL(2,R) \times SL(2,R)$ [10]. Again, this is compatible with the requirements of $N = 2$ worldsheet supersymmetry. We found that some new features emerged, related to the fact that with this choice of real structure (in which pairs of coordinates are grouped together into *double number* quantities, of the form $x + ey$, where $e^2 = +1$, rather than complex quantities $x + iy$, where $i^2 = -1$), quantities that are related by conjugation in the complex case are no longer related in this real basis. This allows certain kinds of additional physical operators at special degenerate momenta that do not arise in the complex basis. There also turn out to be two inequivalent physical degrees of freedom in the theory for generic momenta. In the complex basis, these two states can be related by picture changing and spectral flow, but the situation is more subtle in the real basis, and a description in terms of two genuinely distinct physical states becomes more appropriate [10].

3 p-brane solitons

One of the most dramatic developments in string theory for some years has been the recent understanding of the role of duality symmetries in relating the strong and weak coupling regimes of various string theories, and its implications for the possible unity of all the known string theories as facets of a more fundamental underlying eleven-dimensional theory [11,12]. One of the features of the picture that emerges is that non-perturbative solitonic p-brane states in certain string theories should be interpretable as elementary states in a dual theory. Thus it becomes more and more important to achieve an understanding of the structure of these p-brane solitons in the various theories [13,14,15,16,17,18,19]. Some of my recent work has been focussed in this direction. To begin with, we undertook an investigation of the way in which p-brane solutions in lower-dimensional supergravities, which can be viewed as the low-energy limits of certain string theories compactified on tori, are related to the p-brane solutions of the original ten-dimensional string [20]. By performing the appropriate Kaluza-Klein reduction, one can obtain the lower-dimensional supergravities from the ten-dimensional one. A p-brane solution in D-dimensional supergravity can always be reduced to another p-brane solution (typically with a different value of p) in a lower dimension. Thus some of the lower-dimensional p-branes are nothing but dimensional reductions of higher-dimensional ones. By "factoring out" these examples, and studying what remains, one can build up a classification of the basic p-brane solutions in each dimension, namely the ones that cannot "oxidise" (by the reverse of the process of dimensional reduction) into p-branes in the higher dimension. This classification process was undertaken in [20].

In two recent works, in collaboration with H. Lu, we have carried out a fairly exhaustive classification of all possible p-brane solutions, subject to certain symmetry requirements, in all the maximal supergravities that come from the dimensional reduction of the type IIA theory in $D = 10$, or, equivalently, from $D = 11$ supergravity. In order to do this, we first obtained a complete description, by Kaluza-Klein dimensional reduction, of the bosonic sectors of all the lower-dimensional maximal supergravities, in a formalism adapted to the subsequent analysis [21]. We then showed that the classification problem could be reduced to an exercise in linear algebra. Ultimately, in order to obtain the full results for all possible solutions, including non-supersymmetric as well as supersymmetric ones, it became necessary to use a computer to work through the possibilities. This gave a classification of $SO(1,d-1) \times SO(D-d)$ symmetric $(d-1)$-brane solutions in D dimensions, involving a single dilaton scalar field and a set of antisymmetric-tensor field strengths, all proportional to one-another, with a fixed set of ratios of electric or magnetic charges. We analysed the supersymmetry of all the solutions, using a general method based on computing the eigenvalues of the "Bogomol'nyi matrix" arising as the commutator of conserved supercharges. In

the second paper, we extended these results by constructing generalisations of the supersymmetric solutions, in which the electric or magnetic charges of the field strengths become independent free parameters [22]. These results generalise some previous studies of black holes in four-dimensional string theories [23].

The whole subject of duality in string theory, strong/weak coupling symmetry and the non-perturbative spectrum is a rapidly-developing one, and many advances can be expected in the coming years. There are many possible avenues for investigation, and many fascinating questions arise. One of the most intriguing recent developments is the work on D-branes, *i.e.* open-string theories in which Dirichlet boundary conditions, rather than the usual Neumann conditions, are imposed in some of the spacetime dimensions [24,25,26]. This work gives rise to some hope that progress may finally be made in the understanding of the quantisation of higher-dimensional extended objects, and the role that they have to play in the non-perturbative description of string theory. I am intending to explore some topics in this general area in the near future.

References

[1] C.N. Pope, L.J. Romans and K.S. Stelle, Phys. Let. **B268** (1991) 167; Phys. Lett. **B269** (191) 287.

[2] H. Lu, C.N. Pope, X.J. Wang and K.W. Xu, Class. Quantum Grav. **11** (1994) 967.

[3] H. Lu, C.N. Pope, S. Schrans and X.J. Wang, Nucl. Phys. **B403** (1993) 351; **B408** (1993) 3.

[4] N. Berkovits and C. Vafa, Mod. Phys. Lett. **A9** (1994) 653.

[5] H. Lu, C.N. Pope, K.S. Stelle and K.W. Xu, Phys. Lett. **B351** (1995) 179.

[6] C.N. Pope, L.J. Romans and X. Shen, Phys. Lett. **B236** (1990) 173; Nucl. Phys. **B339** (1990) 191.

[7] S. Krivonos and A. Sorin, Phys. Lett. **B335** (1994) 45.

[8] H. Lu, C.N. Pope and K.W. Xu, Phys. Lett. **B358** (1995) 239.

[9] H. Ooguri and C. Vafa, Mod. Phys. Lett. **A5** (1990) 1389; Nucl. Phys. **B361** (1991) 469.

[10] H. Lu and C.N. Pope, Nucl. Phys. **B447** (1995) 297.

[11] E. Witten, Nucl. Phys. **B443** (1995) 85.

[12] P.K. Townsend, *p-brane democracy*, hep-th/9507048.

[13] A. Dabholkar, G.W. Gibbons, J.A. Harvey and F. Ruiz Ruiz, Nucl. Phys. **B340** (1990) 33.

[14] M.J. Duff and K.S. Stelle, Phys. Lett. **B253** (1991) 113.

[15] M.J. Duff and J.X. Lu, Nucl. Phys. **B354** (1991) 141. R.R. Khuri, Phys. Lett. **307** (1993) 302; R.R. Khuri, Nucl. Phys. **B403** (1993) 335;

[16] C.G. Callan, J.A. Harvey and A. Strominger, Nucl. Phys. **B359** (1991) 611; Nucl. Phys. **B367** (1991) 60; *Supersymmetric String Solitons*, Lectures given at the Trieste Summer School, Trieste, Italy, 1991.

[17] A. Strominger, Nucl. Phys. **B343** (1990) 167; M.J. Duff and J.X. Lu, Phys. Rev. Lett. **66** (1991) 1402.

[18] M.J. Duff, R.R. Khuri and J.X. Lu, Phys. Rep. **259** (1995) 213.

[19] R. Güven, Phys. Lett. **B276** (1992) 49; Phys. Lett. **B212** (1988) 277.

[20] H. Lu, C.N. Pope, E. Sezgin and K.S. Stelle, *Stainless super p-branes*, CTP-TAMU-31/95, hep-th9508042, to appear in Nucl. Phys. B.

[21] H. Lu and C.N. Pope, *p-brane solitons in maximal supergravities*, CTP-TAMU-47/95, hep-th9512012.

[22] H. Lu and C.N. Pope, *Multi-scalar p-brane solitons*, CTP-TAMU-52/95, hep-th9512153.

[23] M. Cvetic and D. Youm, Phys. Lett. **B359** (1995) 87; K. Behrndt, *About a class of exact string backgrounds*, preprint HUB-EP-95/6, hep-th/9506106; R.Kallosh and A. Linde, *Exact supersymmetric massive and massless white holes*, SU-ITP-95-14, hep-th/9507022.

[24] J. Polchinski, *Dirichlet D-branes and Ramond-Ramond charges*, hep-th9510017.

[25] J. Polchinski and E. Witten, *Evidence for heterotic-type I string duality*, hep-th9510169.

[26] P. Horava and E. Witten, *Heterotic and type I string dynamics from eleven dimensions*, hep-th/9510209.

Appendix A

Publications of the Experimental Group for 1995

1. CDF Collaboration (F. Abe *et al.*), "Direct Measurement of the W Boson Width," Physical Review Letters **74**, 341 (1995).

2. CDF Collaboration (F. Abe *et al.*), "Charge Asymmetry in W-Boson Decays Produced in $p\overline{p}$ Collisions at $\sqrt{s} = 1.8$ TeV," Physical Review Letters **74**, 850 (1995).

3. CDF Collaboration (F. Abe *et al.*), "Observation of Rapidity Gaps in $p\overline{p}$ Collisions at 1.8 TeV," Physical Review Letters **74**, 855 (1995).

4. CDF Collaboration (F. Abe *et al.*), "Measurement of W-Photon Couplings in $p\overline{p}$ Collisions at $\sqrt{s} = 1.8$ TeV," Physical Review Letters **74**, 1936 (1995).

5. CDF Collaboration (F. Abe *et al.*), "Limits on Z-Photon Couplings from $p\overline{p}$ Interactions at $\sqrt{s} = 1.8$ TeV," Physical Review Letters **74**, 1941 (1995).

6. CDF Collaboration (F. Abe *et al.*), "Observation of Top Quark Production in $p\overline{p}$ Collisions," Physical Review Letters **74**, 2626 (1995).

7. CDF Collaboration (F. Abe *et al.*), "Search for Charged Bosons Heavier than the W Boson in $p\overline{p}$ Collisions at $\sqrt{s} = 1800$ GeV," Physical Review Letters **74**, 2900 (1995).

8. CDF Collaboration (F. Abe *et al.*), "Search for New Particles Decaying to Dijets in $p\overline{p}$ Collisions at $\sqrt{s} = 1.8$ TeV," Physical Review Letters **74**, 3538 (1995).

9. CDF Collaboration (F. Abe *et al.*), "Measurement of the B_s Meson Lifetime," F. Abe *et al.*, (The CDF Collaboration), Physical Review Letters **74**, 4988 (1995).

10. CDF Collaboration (F. Abe *et al.*), "Measurement of the W Boson Mass," Physical Review Letters **75**, 11 (1995).

11. CDF Collaboration (F. Abe *et al.*), "Properties of High-Mass Multijet Events at the Fermilab Proton-Antiproton Collider," Physical Review Letters **75**, 608 (1995).

12. CDF Collaboration (F. Abe *et al.*), "Search for Squarks and Gluinos via Radiative Decays of Neutralinos in Proton-Antiproton Collisions at $\sqrt{s} = 1.8$ TeV," Physical Review Letters **75**, 613 (1995).

13. CDF Collaboration (F. Abe *et al.*), "Search for Second Generation Leptoquarks in $p\bar{p}$ Collisions at $\sqrt{s} = 1.8$ TeV," Physical Review Letters **75**, 1012 (1995).

14. CDF Collaboration (F. Abe *et al.*), "Limits on WWZ and $WW\gamma$ Couplings from WW and WZ Production in $p\bar{p}$ Collisions at $\sqrt{s} = 1.8$ TeV," Physical Review Letters **75**, 1017 (1995).

15. CDF Collaboration (F. Abe *et al.*), "Measurement of the B Meson Differential Cross Section $d\sigma/dp_T$ in $p\bar{p}$ Collisions at $\sqrt{s} = 1.8$ TeV," Physical Review Letters **75**, 1451 (1995).

16. CDF Collaboration (F. Abe *et al.*), "Search for New Gauge Bosons Decaying into Dielectrons in $\bar{p}p$ Collisions at $\sqrt{s} = 1.8$ TeV," Physical Review D (rapid communication) **51**, 949 (1995).

17. CDF Collaboration (F. Abe *et al.*), "Kinematic Evidence for Top Quark Pair Production in $W+$ Multijet Events in $p\bar{p}$ Collisions at $\sqrt{s} = 1.8$ TeV," Physical Review D (rapid communication) **51**, 4623 (1995).

18. CDF Collaboration (F. Abe *et al.*), "Identification of Top Quarks using Kinematic Variables," Physical Review D (rapid communication) **52**, 2605 (1995).

19. CDF Collaboration (F. Abe *et al.*), "Measurement of the Ratio $\sigma B(p\bar{p} \to W \to e\nu)/\sigma B(p\bar{p} \to Z^0 \to ee)$ in $p\bar{p}$ Collisions at $\sqrt{s} = 1800$ GeV," Physical Review D **52**, 2624 (1995).

20. T. Kamon *et al.* (CDF Collaboration), "Search for SUSY at CDF," Proceedings of the Eighth Meeting of the Division of Particles and Fields, Ed. S. Seidel (World Scientific) Vol. 2, p. 1056 (1995).

21. J. Strait *et al.*, "Tevatron Energy and Luminosity Upgrades Beyond the Main Injector," to appear in Proceedings of the Eighth Meeting of the Division of Particles and Fields, Ed. S. Seidel (World Scientific) Vol. 2, p. 1451 (1995).

22. H.-J. Trost *et al.*, "Gas Microstrip Chambers with Two-Dimensional Readout," to appear in Proceedings of the Eighth Meeting of the Division of Particles and Fields, Ed. S. Seidel (World Scientific) Vol. 2, p. 1924 (1995).

23. T. Kamon (CDF Collaboration), "Search for SUSY at CDF," Proceedings of Beyond the Standard Model IV, Ed. J.F. Gunion, T. Han, and J. Ohnemus, (World Scientific) p. 546 (1995).

24. "$b\bar{b}$ Quark Pair Correlations in $\overline{p}p$ Collisions at $\sqrt{s} = 1.8$ TeV," F. Abe *et al.* (CDF Collaboration), Fermilab-Pub-94/131-E, submitted to Physical Review Letters (1994).

25. CDF Collaboration (F. Abe *et al.*), "Analysis of Jet Charged Particle Momentum Distributions for Quark-gluon Separation in $\overline{p}p$ Collisions at $\sqrt{s} =$ 1.8 TeV," Fermilab-Pub-94/171-E, submitted to Physical Review D (1994).

26. CDF Collaboration (F. Abe *et al.*), "Measurement of $W + \gamma$ and $Z + \gamma$ Cross Sections in the Electron and Muon Channels in $p\overline{p}$ Collisions at $\sqrt{s} = 1.8$ TeV," Fermilab-Pub-94/244-E, submitted to Physical Review D (1994).

27. "Measurement of the W Boson Mass," F. Abe *et al.* (CDF Collaboration), Fermilab-Pub-95/033-E; submitted to Physical Review D (1995).

28. F. Abe *et al.* (CDF Collaboration), "Measurement of Correlated $\mu - \bar{b}$ jet Cross Sections in $p\overline{p}$ Collisions at $\sqrt{s} = 1.8$ TeV," Fermilab-Pub-95/289-E; submitted to Physical Review D (1995).

29. M. Ambrosio *et al.* (MACRO Collaboration), " Estimate of Primary Cosmic Ray Composition from a Multi-parametric Fit of MACRO Multimuons Events ", Paper submitted to the ICRC, Rome Meeting, September, 1995.

30. M. Ambrosio *et al.* (MACRO Collaboration), "MACRO Absolute Muon Flux Measurament: Comparison with Monte Carlo Predictions" Paper submitted to the ICRC, Rome Meeting, September, 1995.

31. M. Ambrosio *et al.* (MACRO Collaboration), " Search for Fast Magnetic Monopoles with the MACRO Scintillator System", Paper submitted to the ICRC, Rome Meeting, September, 1995.

32. M. Ambrosio *et al.* (MACRO Collaboration), " Search for GUT Monopoles with the MACRO Streamer Tube and Track Etch System", Paper submitted to the ICRC, Rome Meeting, September, 1995.

33. M. Ambrosio *et al.* (MACRO Collaboration), " Muon Astronomy and Seasonal Variations of the Underground Muon Flux with MACRO", Paper submitted to the ICRC, Rome Meeting, September, 1995.

34. M. Ambrosio *et al.* (MACRO Collaboration), " Study of Primary Interactions with Multiple Muon Events in MACRO", Paper submitted to the ICRC, Rome Meeting, September, 1995.

35. M. Ambrosio *et al.* (MACRO Collaboration), " Sensitivity of MACRO to U.H.E. Neutrinos", Paper submitted to the ICRC, Rome Meeting, September, 1995.

36. M. Ambrosio *et al.* (MACRO Collaboration), " Performance of Transition Radiation Detector in MACRO", Paper submitted to the ICRC, Rome Meeting, September, 1995.

37. M. Ambrosio *et al.* (MACRO Collaboration), " Upward-going Muons in MACRO", Paper submitted to the ICRC, Rome Meeting, September, 1995.

38. M. Ambrosio *et al.* (MACRO Collaboration), " Vertical Muon Intensity Measured with MACRO at the Gran Sasso Laboratory", Phys. Rev. **D52**, 3793(1995).

39. E. Ables *et al.* (MINOS Collaboration), " P-875: A Long Baseline Neutrino Oscillation Experiment at Fermilab", Fermilab-Proposal-P-875, February, 1995.

40. M. Ambrosio *et al.* (MACRO Collaboration), " Performance of the MACRO Streamer Tube System in the Search for Magnetic Monopoles", Astroparticle Physics, 4, 33(1995).